Inorganic Chemistry

Article

pubs.acs.org/IC

Synthesis and Coordination Chemistry of Phosphine Oxide Decorated Dibenzofuran Platforms

Daniel Rosario-Amorin,[†] Eileen N. Duesler,[†] Robert T. Paine,*[,†] Benjamin P. Hay,[‡] Lætitia H. Delmau,[‡] Sean D. Reilly,[§] Andrew J. Gaunt,*[,§] and Brian L. Scott[∥]

[†]Department of Chemistry and Chemical Biology, University of New Mexico, Albuquerque, New Mexico 87131, United States

[‡]Chemical Sciences Division, Oak Ridge National Laboratory, P.O. Box 2008, Oak Ridge, Tennessee 37831, United States

[§]Chemistry Division and [∥]Materials Physics and Applications Division, Los Alamos National Laboratory, Los Alamos, New Mexico 87545, United States

Supporting Information

ABSTRACT: A four-step synthesis for 4,6-bis(diphenylphosphinoylmethyl)-dibenzofuran (**4**) from dibenzofuran and a two-step synthesis for 4,6-bis-(diphenylphosphinoyl)dibenzofuran (**5**) are reported along with coordination chemistry of **4** with In(III), La(III), Pr(III), Nd(III), Er(III), and Pu(IV) and of **5** with Er(III). Crystal structure determinations for the ligands, **4**·CH_3OH and **5**, the 1:1 complexes $[In(\mathbf{4})(NO_3)_3]$, $[Pr(\mathbf{4})(NO_3)_3(CH_3CN)]\cdot 0.5CH_3CN$, $[Er(\mathbf{4})(NO_3)_3(CH_3CN)]\cdot CH_3CN$, $[Pu(\mathbf{4})Cl_4]\cdot THF$ and the 2:1 complex $[Nd(\mathbf{4})_2(NO_3)_2]_2(NO_3)_2\cdot(H_2O)\cdot 4(CH_3OH)$ are described. In these complexes, ligand **4** coordinates in a bidentate POP′O′ mode via the two phosphine oxide O-atoms. The dibenzofuran ring O-atom points toward the central metal cations, but in every case it is more than 4 Å from the metal. A similar bidentate POP′O′ chelate structure is formed between **5** and Er(III) in the complex, $\{[Er(\mathbf{5})_2(NO_3)_2](NO_3)\cdot 4(CH_3OH)\}_{0.5}$, although the nonbonded Er···O_{furan} distance is reduced to ∼3.6 Å. The observed bidentate chelation modes for **4** and **5** are consistent with results from molecular mechanics computations. The solvent extraction performance of **4** and **5** in 1,2-dichloroethane for Eu(III) and Am(III) in nitric acid solutions is described and compared against the extraction behavior of *n*-octyl(phenyl)-*N*,*N*-diisobutylcarbamoylmethyl phosphine oxide (OΦDiBCMPO) measured under identical conditions.

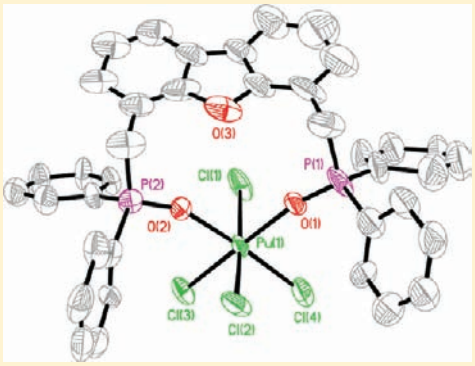

INTRODUCTION

A variety of organic platforms have been utilized to append donor groups in geometrically favorable arrangements so that the resulting molecules generate either strongly chelating or hemilabile coordination fields for metal cations. Although not largely popular, the rigid 4,6-dibenzofuran (4,6-DBF) fragment is one such platform that has been used to create interesting acyclic[1−15] and macrocyclic[16−20] ligands. Reports on the coordination chemistry of these ligands are few, but where structural data are available, it has been observed that the DBF O-atom may participate in chelate formation[2,3,6,12,14] or not.[4,7−9] In previous ligand construction activities we have used 2-pyridine N-oxide (2-XC_5H_4NO) and/or 2,6-pyridine N-oxide (2,6-$X_2C_5H_3NO$) ring platforms to attach donor functionalized substituent arms, X = phosphine oxide, -$[P(O)R_2]$,[21,22] phosphonate, -$[P(O)(OR)_2]$,[23] methylphosphine oxide, -$[CH_2P(O)R_2]$,[24−33] methylphosphonate, -$[CH_2P(O)(OR)_2]$,[34] methylphosphinic acid, -$CH_2P(O)(OH)_2$],[34] methylphosphine sulfide, -$[CH_2P(S)R_2]$[35] and methylamido, -$[CH_2C(O)N(H)R]$[36] and −$[CH_2CH_2C(O)NR_2]$.[37] Generally, the 2-XC_5H_4NO compounds behave as bidentate, chelating NOPO[24,33] or NOCO[37] ligands toward hard metal cations, while the 2,6-$(X)_2C_5H_3NO$ compounds act as tridentate NOPOP′O[21−27] or NOCOC′O′ chelates. Furthermore, examples of the NOPOP′O′ class display useful solvent extraction properties for trivalent *f*-block element cations.[38−41] Our continuing interest in developing new chelating conditions, especially for *f*-block metal cations, has led us to explore the possibility of using phosphine oxide and methyl phosphine oxide donor centers to decorate the 4,6-DFB fragment, and determine if the resulting ligands utilize the DBF ring O-atom in coordination interactions with hard cations. The syntheses for these ligands, molecular modeling of potential coordination interactions, selected coordination chemistry toward hard acceptor ions, In(III), Ln(III) (Ln = La, Pr, Nd, and Er) and Pu(IV), and a survey of the liquid−liquid solvent extraction properties with Eu(III) and Am(III) are described in this report.

EXPERIMENTAL SECTION

General Information. Organic reagents (Aldrich Chemical Co) and metal nitrates (Ventron) were used as received, and organic solvents (VWR) were dried and distilled by standard methods. ***Caution!*** *All plutonium chemistry was conducted at Los Alamos National Laboratory inside specialist radiological facilities designed for the safe handling and manipulation of high specific-activity α-particle emitting*

Received: February 10, 2012
Published: June 7, 2012

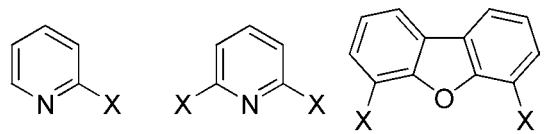

2-XC_5H_4NO 2,6-$X_2C_5H_3NO$ 4,6-X_2DBF

radionuclides. The plutonium(IV) solution (0.46 M in aqueous HCl, isotopic composition: 94% ^{239}Pu, 6% ^{240}Pu, trace ^{238}Pu, ^{240}Pu, and ^{242}Pu) was purified by using anion-exchange chromatography. The plutonium solution concentration and oxidation state were determined by measuring the vis−NIR spectrum of a solution sample diluted in 1.0 M $HClO_4$. Reactions were performed under dry nitrogen unless specified otherwise. Infrared spectra were recorded on a Bruker Tensor 27 benchtop spectrometer. A Varian Cary 6000i spectrophotometer with a fixed spectral bandwidth of 0.2 nm was used to record solution electronic absorption spectra at ambient temperature. Solid diffuse reflectance spectra were collected using a Varian Cary 500 with installed Internal Diffuse Reflectance Accessory. Solution NMR spectra were measured with Bruker FX-250 and Avance-300 and -500 spectrometers using Me_4Si (^1H, ^{13}C) and 85% H_3PO_4 (^{31}P) as external standards. Downfield shifts from the reference resonances were given $+\delta$ values. The atom numbering systems used for the NMR resonance assignments are provided on spectral traces included in the Supporting Information. The Pu(IV) solutions were contained inside 4 mm diameter PTFE NMR tube liners to provide multiple containment of the radioactive isotopes. The high resolution mass spectra were obtained at the UNM Mass Spectrometry Center by using electrospray ionization (ESI) with a Waters/Micromass mass spectrometer. Elemental analyses (CHN) were performed by Galbraith Laboratories.

Ligand Syntheses. *4,6-Diformyl-dibenzofuran (**1**).* An aliquot of *n*-butyllithium (1.6 M in hexane, 46.4 mL, 74.3 mmol) was added to dibenzofuran (5 g, 30 mmol) and *N,N,N′,N′*-tetramethylethylenediamine (11.1 mL, 74.3 mmol) in dry hexane (30 mL). The resulting mixture was refluxed (10 min), cooled (0 °C), and DMF (10 mL) was added. This mixture was allowed to slowly warm (23 °C, 1 h) while stirring, and then quenched with water (20 mL). The resulting solid was collected by filtration, washed with water (3 × 20 mL), and crystallized from hot methanol leaving a bone-white powder, **1**: yield 1.8 g, 27%; mp 218−220 °C. ^1H NMR (500 MHz, $CDCl_3$): δ 10.71 (s, 2H, H_1), 8.25 (d, J_{HH} = 8.0 Hz, 2H, H_5), 8.05 (d, J_{HH} = 8.0 Hz, 2H, H_3), 7.56 (t, J_{HH} = 7.5 Hz, 2H, H_4). $^{13}C\{^1H\}$ NMR (125.8 MHz, $CDCl_3$): δ 187.62 (C_1), 156.51 (C_7), 127.86 (C_5), 126.86 (C_3), 124.74 (C_6), 123.97 (C_4), 121.65 (C_2). HRMS(ESI): *m*/*z* (%): 247.0371 [M+Na$^+$] (100). $C_{14}H_8NaO_3$ requires 247.0367.

*4,6-Bis(hydroxymethyl)-dibenzofuran (**2**).* To a suspension of **1** (1.78 g, 7.94 mmol) in MeOH/$CHCl_3$ (1/1, 40 mL), was added $NaBH_4$ (587 mg, 15.5 mmol), and the mixture was stirred (23 °C, 12 h) under nitrogen. The mixture was concentrated to 10 mL, and water (20 mL) was added. The resulting pale yellow solid, **2**, was collected by filtration: yield 1.6 g, 88%; mp 188−190 °C. ^1H NMR (300 MHz, $CDCl_3$): δ 7.92 (d, J_{HH} = 7.2 Hz, 2H, H_5), 8.05 (d, J_{HH} = 7.5 Hz, 2H, H_3), 7.38 (t, J_{HH} = 7.5 Hz, 2H, H_4) 5.13 (d, J_{HH} = 6.3 Hz, 4H, H_1). $^{13}C\{^1H\}$ NMR (125.8 MHz, d_6-DMSO): δ 151.26 (C_7), 124.89 (C_3), 124.50 (C_2), 121.60 (C_4), 121.59 (C_6), 118.10 (C_5), 56.14 (C_1). FTIR (KBr, cm^{-1}): 1489, 1432, 1366, 1190, 1074, 1050, 1028, 991, 869, 842, 806, 766, 741, 669, 610. HRMS(ESI): *m*/*z* (%): 251.0684 [M+Na$^+$] (100). $C_{14}H_{12}NaO_3$ requires 251.0677.

*4,6-Bis(chloromethyl)-dibenzofuran (**3**).* Under dry nitrogen, a suspension of **2** (780 mg, 3.41 mmol) and triphenylphosphine (2.68 g, 10.3 mmol) in dry CH_2Cl_2 (50 mL) was cooled (0 °C) and N-chlorosuccinimide (1.36 g, 10.3 mmol) was added. Stirring was continued (0 °C) until the mixture became homogeneous, and then the solution was warmed (23 °C) and stirred (12 h). The solvent was vacuum evaporated, and the residue was purified by column chromatography (silica gel, eluted with hexane/Et_2O, 95/5). Following vacuum evaporation of the eluant, compound **3** was obtained as a yellow powder: yield 830 mg, 92%; mp 136−138 °C. ^1H NMR (500 MHz, $CDCl_3$): δ 7.88 (d, J_{HH} = 7.5 Hz, 2H, H_5), 7.52 (d, J_{HH} = 7.0 Hz, 2H, H_3), 7.35 (t, J_{HH} = 7.5 Hz, 2H, H_4), 5.00 (d, J_{HH} = 6.3 Hz, 4H, H_1). $^{13}C\{^1H\}$ NMR (125.8 MHz, $CDCl_3$): δ 153.88 (C_7), 128.00 (C_3), 124.49 (C_2), 123.40 (C_4), 121.81 (C_6), 121.22 (C_5), 40.27 (C_1). FTIR (KBr, cm^{-1}): 1488, 1433, 1420, 1352, 1326, 1263, 1224, 1188, 1118, 1057, 864, 844, 803, 781, 745, 667, 612, 578, 542. HRMS(ESI): *m*/*z* (%): 229.0412 [M-Cl$^+$] (100). $C_{14}H_{10}ClO$ requires 229.0420. Anal. Calcd for $C_{14}H_{10}Cl_2O$: C 63.42, H 3.80. Found: C 63.74, H 4.21.

*4,6-Bis(diphenylphosphinoylmethyl)-dibenzofuran (**4**).* A solution of **3** (630 mg, 2.38 mmol) in ethyl diphenylphosphinite (3 mL, 13.9 mmol) was refluxed under nitrogen until the solution solidified. The solid was heated (120 °C, 12 h), and the resulting white residue was collected and washed with diethyl ether (3 × 10 mL) giving **4** as a white powder: yield 1.37 g, 96%; mp 238−240 °C. $^{31}P\{^1H\}$ NMR (202.1 MHz, $CDCl_3$): δ 29.8; (MeOH-d_4): δ 34.5. ^1H NMR (500 MHz, $CDCl_3$): δ 7.8−7.7 (m, 10H, $H_{5,9}$), 7.45−7.35 (m, 4H, H_{11}) 7.45−7.35 (m, 10H, $H_{3,10}$), 7.19 (t, J_{HH} = 8.0 Hz, 2H, H_4), 3.91 (d, J_{PH} = 13.5 Hz, 4H, H_1). $^{13}C\{^1H\}$ NMR (125.8 MHz, $CDCl_3$): δ 154.28 (d, J_{CP} = 5.2 Hz, C_7), 132.49 (d, J_{CP} = 98.7 Hz, C_8), 131.91 (C_{11}), 131.16 (d, J_{CP} = 9.1 Hz, C_9), 128.90 (d, J_{CP} = 5.2 Hz, C_3), 128.47 (d, J_{CP} = 11.5 Hz, C_{10}), 124.11 (C_6), 123.02 (C_4), 119.44 (C_5), 115.57 (d, J_{CP} = 7.2 Hz, C_2), 31.81 (d, J_{CP} = 66.9 Hz, C_1). FTIR (KBr, cm^{-1}): 3431, 3056, 2944, 2904, 1632, 1591, 1487, 1436, 1408, 1328, 1262, 1191(ν_{PO}), 1174, 1120, 1071, 1051, 1029, 998, 885, 851, 832, 806, 782, 743, 725, 694, 569, 536, 512, 462, 407. HRMS(ESI): *m*/*z* (%): 597.1742 [M+H$^+$] (35). $C_{38}H_{31}O_3P_2$ requires 597.1748; 619.1559 [M+Na$^+$] (100). $C_{38}H_{30}O_3NaP_2$ requires 619.1568. Anal. Calcd for $C_{38}H_{30}O_3P_2$: C 76.50, H 5.07. Found: C 75.68, H 5.03.

*4,6-Bis(diphenylphosphinoyl)-dibenzofuran (**5**). **Method A**.* Under dry nitrogen, a solution of *n*-BuLi (1.6 M in hexane, 9.3 mL, 15 mmol) was combined with dibenzofuran (1 g, 6 mmol) and *N,N,N′,N′*-tetramethylethylenediamine (2.2 mL, 15 mmol) in dry hexane (20 mL), and the combination refluxed (10 min). The mixture was cooled (0 °C), and diphenylphosphinic chloride (2.32 mL, 11.9 mmol) was added. The resulting mixture was slowly warmed (23 °C) over 2 h, stirred, and then quenched with water (20 mL). The resulting solid was collected by filtration and washed with water (3 × 20 mL). The residue was dissolved in a minimum amount of MeOH, precipitated by addition of Et_2O and washed with Et_2O (3 × 10 mL). The bone-white powder obtained was purified by column chromatography (silica gel eluted with CH_2Cl_2/MeOH 98/2) leaving **5** as a white powder: yield 620 mg, 18%; mp >380 °C (dec). ***Method B***. Under dry nitrogen, a solution of *n*-BuLi (1.6 M in hexane, 40.5 mL, 64.8 mmol) in hexane (80 mL) was added dropwise (40 m, 23 °C) to a solution of dibenzofuran (3.36 g, 20.0 mmol) and *N,N,N′,N′*-tetramethylethylenediamine (9.78 mL, 64.8 mmol) in dry hexane (80 mL). After addition, the resulting mixture was refluxed (1 h), then cooled (0 °C), and a solution of Ph_2PCl (7.20 mL, 40.0 mmol) in hexane (50 mL) was added (1 h). The mixture was stirred (23 °C, 12 h), then quenched with water (10 mL), and the combination concentrated in vacuo. The residue was extracted with CH_2Cl_2 (3 × 30 mL), the organic layer recovered, dried ($MgSO_4$), hydrogen peroxide (30%, 10 mL) added, and the mixture stirred (23 °C, 3 h). The resulting mixture was treated with water (20 mL), and the phases separated. The organic fraction was dried ($MgSO_4$), filtered and the solvent removed in vacuo leaving a brown residue that was treated with Et_2O (50 mL). The resulting pale yellow solid was collected by filtration and washed with Et_2O. This solid was dissolved in CH_2Cl_2, filtered through a silica pad, and the volatiles evaporated in vacuo providing **5** as a white powder (3.6 g). Additional product was recovered by vacuum evaporation of the combined ether filtrate and wash phases, and the residue purified by column chromatography (silica gel, elution with CH_2Cl_2/MeOH 98/2) leaving a white powder, **5** (2.1 g): combined yield 5.7 g, 50%; mp >380 °C (dec). $^{31}P\{^1H\}$ NMR (121.49 MHz, $CDCl_3$): δ 25.2. ^1H NMR (300 MHz, $CDCl_3$): δ 8.15 (d, J_{HH} = 7.5 Hz, 2H, H_4), 7.82−7.76 (m, 2H, H_2) 7.67−7.60 (m, 8H, H_8), 7.45−7.36 (m, 6H, $H_{3,10}$), 7.36−7.28 (m, 8H, H_9). $^{13}C\{^1H\}$ NMR (75.4 MHz, $CDCl_3$) δ 156.23 (C_6), 133.01 (d, J_{CP} = 6.1 Hz, C_2), 132.13 (s, C_{10}), 131.90 (d, J_{CP} = 10.6 Hz, C_8), 131.79 (d, J_{CP} = 107.6 Hz, C_7), 128.58 (d, J_{CP} = 12.6 Hz, C_9), 125.03 (s, C_3), 124.15 (d, J_{CP} = 6.2 Hz, C_5), 123.42 (d, J_{CP} = 10.6 Hz, C_4), 117.00 (d, J_{CP} = 100.2 Hz, C_1). FTIR (KBr, cm^{-1}): 3430, 1573, 1470, 1437, 1413, 1393, 1181 (ν_{PO}), 1122, 899, 837, 811, 787, 742,

dx.doi.org/10.1021/ic300301d | *Inorg. Chem.* 2012, 51, 6667−6681

724, 694, 588, 574, 559, 547, 533, 497. HRMS(ESI): *m/z* (%): 569.1428 [M+H$^+$] (40). $C_{36}H_{27}O_3P_2$ requires 569.1435; 591.1232 [M+Na$^+$] (100). $C_{36}H_{26}O_3NaP_2$ requires 591.1255.

Syntheses of Metal Complexes. *Indium and Lanthanide Complexes of* ***4****.* Solutions of $In(NO_3)_3$ and $Ln(NO_3)_3{\cdot}xH_2O$ (84 μmol, 1 equiv) in MeOH/EtOAc (1/1, 2 mL) were added dropwise to solutions of ligand **4** (50−100 mg, 84−168 μmol, 1−2 equiv) in MeOH/EtOAc (1/1, 3 mL). The mixtures were stirred (23 °C, 1 h), and the resulting clear solutions were evaporated to dryness leaving solid residues. *[In(**4**)(NO$_3$)$_3$].* $^{31}P\{^1H\}$ NMR (121.5 MHz, $CDCl_3$): δ 29.7; (MeOH-d_4): δ 35.1. ^1H NMR (300 MHz, $CDCl_3$): δ 7.74−7.69 (m, 10H, $H_{5,9}$), 7.61−7.28 (m, 14H, $H_{3,10,11}$), 7.25 (m, 2H, H_4), 3.88 (d, J_{HH} = 15.0 Hz, 4H, H_1). ^1H NMR (300 MHz, MeOH-d_4): 7.78−7.72 (m, 10H, $H_{5,9}$), 7.56−7.47 (m, 12H, $H_{10,11}$), 7.16−7.15 (m, 4H, $H_{3,4}$), 4.12 (d, J_{HH} = 12.9 Hz, 4H, H_1). FTIR (KBr, cm^{-1}): 3057, 2912, 1591, 1527, 1495, 1439, 1397, 1294, 1273, 1250, 1200, 1163, 1140(ν_{PO}), 1124, 1095, 1011, 887, 849, 827, 802, 787, 764, 741, 727, 689, 623, 532, 513, 501. Anal. Calcd for [In(**4**)(NO$_3$)$_3$], $C_{38}H_{30}InN_3O_{12}P_2$: C, 50.86; H, 3.37; for [In(**4**)$_2$(NO$_3$)$_3$], $C_{76}H_{60}InN_3O_{15}P_4$: C, 61.10; H, 4.05. Found: C, 58.73; H, 4.10. *[La(**4**)(NO$_3$)$_3$]·H$_2$O.* $^{31}P\{^1H\}$ NMR (121.5 MHz, MeOH-d_4): δ 35.6. ^1H NMR (300 MHz, MeOH-d_4): δ 7.72−7.68 (m, 10H, $H_{5,9}$), 7.53−7.39 (m, 12H, $H_{10,11}$), 7.14−7.09 (m, 4H, $H_{3,4}$), 4.07 (d, J_{HH} = 13.8 Hz, 4H, H_1). FTIR (KBr, cm^{-1}): 3059, 2916, 1628, 1591, 1469, 1437, 1296, 1190, 1159, 1142 (ν_{PO}), 1094, 1028, 997, 883, 847, 818, 791, 733, 695, 625, 559, 532, 513. Anal. Calcd for [La(**4**)(NO$_3$)$_3$]·H$_2$O, $C_{38}H_{32}LaN_3O_{13}P_2$: C, 48.58; H, 3.43. Found: C, 48.55; H 3.55. *[Pr(**4**)(NO$_3$)$_3$]·H$_2$O.* $^{31}P\{^1H\}$ NMR (121.5 MHz, DMF-d_7): δ 34.6 (br). ^1H (300 MHz, DMF-d_7): δ 8.12−8.03 (m, 8H, H_9), 7.82 (d, J_{HH} = 7.2 Hz, 2H, H_5), 7.58−7.56 (m, 12H, $H_{10,11}$), 7.35 (d, J_{HH} = 6.9 Hz, 2H, H_3), 7.14 (d, J_{HH} = 6.9 Hz, 2H, H_4), 4.5 (br, 4H, H_1). FTIR (KBr, cm^{-1}): 3059, 2918, 1730, 1684, 1591, 1491, 1437, 1298, 1190, 1167, 1142 (ν_{PO}), 1122, 1095, 1028, 999, 885, 847, 814, 791, 733, 692, 579, 561, 532, 513. Anal. Calcd for [Pr(**4**)(NO$_3$)$_3$]·H$_2$O, $C_{38}H_{32}N_3O_{13}P_2Pr$: C 48.48, H 3.43. Found: C, 48.36; H, 3.52. *[Er(**4**)(NO$_3$)$_3$]·H$_2$O.* FTIR (KBr, cm^{-1}): 3059, 2914, 1732, 1684, 1591, 1473, 1437, 1296, 1190, 1150, 1140 (ν_{PO}), 1122, 1094, 1028, 997, 885, 847, 818, 791, 734, 692, 579, 561, 532, 513. *[Nd(**4**)$_2$(NO$_3$)$_3$]·H$_2$O.* FTIR (KBr, cm^{-1}): 3057, 2916, 1591, 1484, 1437, 1304, 1194, 1143 (ν_{PO}), 1122, 1095, 1052, 1027, 998, 887, 847, 819, 789, 738, 694, 626, 578, 534, 512. Anal. Calcd for [Nd(**4**)$_2$(NO$_3$)$_2$](NO$_3$)·H$_2$O, $C_{76}H_{62}NdN_3O_{16}P_4$: C, 59.46; H, 4.15. Found: C, 59.40; H, 4.18.

Erbium Complex of ***5****.* A solution of $Er(NO_3)_3{\cdot}5H_2O$ (88 μmol, 1equiv) in MeCN/MeOH (4/1, 3 mL) was added dropwise to a solution of ligand **5** (50 mg, 88 μmol, 1 equiv) in MeOH/EtOAc (1/1, 3 mL). The resulting mixture was stirred (23 °C, 1 h), and the clear solution was evaporated to dryness leaving a solid residue. *[Er(**5**)$_2$(NO$_3$)$_3$]·4H$_2$O.* FTIR (KBr, cm^{-1}): 2924, 2854, 1591, 1472, 1439, 1418, 1300, 1203, 1150 (ν_{PO}), 1122, 1097, 1030, 903, 839, 816, 783, 744, 731, 690, 592, 559, 546, 528, 507. Anal. Calcd for [Er(**5**)$_2$(NO$_3$)$_2$]·4H$_2$O, $C_{72}H_{60}ErN_3O_{19}P_4$: C, 55.35; H, 3.87. Found: C, 55.33; H, 3.65.

Plutonium Complex of ***4****. **Method 1**.* Aqueous Pu(IV)/HCl solution (9.1 μL, 4.2 μmol Pu) was added to tetrahydrofuran (THF, 700 μL), and this solution was combined with a sample of **4** (2.9 mg, 4.9 μmol) in MeOH (750 μL). The vial was sealed and left to stand. After 6 days, the vial cap was loosened to allow solvent to slowly evaporate. Crystals formed in the vial by the following day, and these were used in the X-ray diffraction and the vis−NIR spectroscopic analyses. ***Method 2***. A sample of **4** (4.6 mg, 7.7 μmol) was dissolved in THF (1 mL), and combined with aqueous Pu(IV)/HCl solution (18.2 μL, 8.37 μmol Pu). Vapor diffusion of Et_2O into the THF solution produced a yellow powder that was air-dried: yield 5 mg, 66%. This solid was found to be insoluble or sparingly soluble in THF, CH_2Cl_2, EtOH, EtOAc, MeCN, and acetone, and it was used for the diffuse reflectance vis−NIR analysis. *Pu(IV)-**4** spectrophotometric titration*: Aqueous Pu(IV)/HCl solution (9.1 μL, 4.2 μmol Pu) was added to THF (700 μL), and a vis−NIR spectrum of the clear yellow solution was recorded. A sample of **4** (4.6 mg, 7.7 μmol) in THF (1.0 mL) was added in aliquots, and the vis−NIR spectrum was recorded after each addition. As **4** was added, the solution turned a paler yellow color. *NMR of Pu(IV)-**4** solution complex*: A sample of **4** (4.2 mg, 7.0 μmol) was dissolved in THF-d_8 (1 mL), and the ^{31}P and ^1H NMR spectra were recorded. Aqueous Pu(IV)/HCl solution (17.3 μL, 7.96 μmol Pu) was then added to the ligand solution, and the ^{31}P NMR (referenced to external 85% H_3PO_4) and ^1H NMR (referenced to residual internal solvent protio resonances) spectra were recorded. ^1H NMR (THF-d_8, 25 °C, 300 MHz): δ 8.10 (br, 2H, benzo-*H*), 7.59 and 7.40 (br, 20H, phenyl-*H*), 7.00 (t, 2H, benzo-*H*), 6.32 (br, 2H, benzo-*H*), 4.79 (excess protons from Pu(IV)/HCl stock solution aliquot addition), 3.58 and 1.73 (residual protio resonances from THF-d_8). $^{31}P\{^1H\}$ NMR (THF-d_8, 25 °C, 300 MHz): δ 0.58.

X-ray Diffraction Analyses. Crystals of the ligands and lanthanide and indium complexes were placed in glass capillaries and mounted on a Bruker X8 APEX II CCD-based X-ray diffractometer located at UNM that is equipped with an Oxford Cryostream 700 low temperature device and normal focus Mo-target X-ray tube (λ = 0.71073 Å). Crystals of the plutonium complex were contained in paratone and a wax-sealed quartz capillary coated in acrylic. The diffraction data were collected with a Bruker D8 diffractometer outfitted with an APEX II CCD detector and Bruker Kryoflex low temperature device located at LANL. The instrument was equipped with a graphite monochromatized Mo Kα X-ray source (λ = 0.71073 Å) and a 0.5 mm monocapillary. The data frames were integrated with the Bruker SAINT software package[42] and absorption corrections were applied with SADABS.[43] In no case was crystal decay observed. The structures were solved and refined by direct methods and difference Fourier techniques using the Bruker SHELXTL software package.[44] Lattice and data collection parameters for the ligands and the metal complexes are presented in Tables 1 and 2, respectively.

Table 1. Crystallographic Data for Ligands 4·CH$_3$OH and 5

	4·CH$_3$OH	5
empirical formula	$C_{39}H_{34}O_4P_2$	$C_{36}H_{26}O_3P_2$
crystal size (mm)	0.21 × 0.22 × 0.39	0.08 × 0.18 × 0.32
formula weight	628.60	568.51
crystal system	triclinic	monoclinic
space group	*P*1	$P2_1/n$
unit cell dimen.		
a (Å)	11.1295(3)	13.3352(2)
b (Å)	12.1172(3)	11.0946(2)
c (Å)	13.6427(3)	18.8531(3)
α (deg)	88.335(1)	90
β (deg)	69.154(1)	94.015(1)
γ (deg)	76.794(1)	90
V (Å^3)	1671.17(7)	2782.45(8)
Z	2	4
T, (K)	150(2)	150(2)
D_{cald} (g cm^{-3})	1.249	1.357
μ(mm^{-1})	0.170	0.194
min/max transmission	0.9365/0.9654	0.9402/0.9845
reflection collected	40022	61938
independent reflections [R_{int}]	11076[0.0150]	9199[0.0296]
final R indices [$I > 2\sigma(I)$] R1 (*w*R2)	0.0393(0.1058)	0.0407(0.1038)
final R indices (all data) R1(*w*R2)	0.0489(0.1145)	0.0573(0.1140)

All heavy atoms were refined anisotropically, and all carbon hydrogen atoms were included in ideal positions and refined isotropically (riding model) with U_{iso} = 1.2U_{eq} of the parent atom unless noted otherwise. The structure refinements were well behaved except as indicated in the following notes. *4·CH$_3$OH*: colorless prisms were obtained by dissolving 100 mg of **4** in MeOH/CH_2Cl_2 (1/1, 10 mL), concentrating this solution until cloudy (~5 mL), adding a few drops of CH_2Cl_2, and holding the resulting solution at −20 °C (12 h). The MeOH lattice solvent molecule is disordered over two positions with occupancies set at 51.73% (O1s,C1s) and 48.27% (O2s, C2s). The H-atoms on the O- and

dx.doi.org/10.1021/ic300301d | *Inorg. Chem.* 2012, 51, 6667−6681

Table 2. Crystallographic Data for Coordination Complexes

	[In(**4**)$(NO_3)_3$]	[Pr(**4**)$(NO_3)_3(CH_3CN)$]·0.5(CH_3CN)	[Er(**4**)$(NO_3)_3(CH_3CN)$]·(CH_3CN)	[Nd(**4**)$_2(NO_3)_2]_2(NO_3)_2$·(H_2O)·4(CH_3OH)	[Pu(**4**)Cl_4]·(THF)	{[Er(**5**)$_2(NO_3)_2$](NO_3)·4 $CH_3OH\}_{0.5}$
empirical formula	$C_{38}H_{30}InN_3O_{12}P_2$	$C_{41}H_{34.5}N_{4.5}O_{12}P_2Pr$	$C_{42}H_{36}ErN_5O_{12}P_2$	$C_{156}H_{138}N_6Nd_2O_{35}P_8$	$C_{42}H_{34}O_4P_2Cl_4Pu$	$C_{38}H_{34}Er_{0.5}N_{1.5}O_{9.5}P_2$
crystal size (mm)	0.21 × 0.25 × 0.05	0.50 × 0.30 × 0.20	0.41 × 0.32 × 0.07	0.41 × 0.18 × 0.09	0.21 × 0.25 × 0.05	0.37 × 0.32 × 0.31
formula weight	897.41	985.08	1031.96	3192.96	1045.49	809.24
crystal system	monoclinic	monoclinic	monoclinic	monoclinic	monoclinic	monoclinic
space group	$P2_1/n$	$P2_1/n$	$C2/c$	$P2_1/c$	$C2/c$	$C2/c$
unit cell dimen.						
a (Å)	9.3835(5)	10.6540(4)	29.527(2)	36.938(2)	20.108(5)	18.9860(6)
b (Å)	23.475(1)	15.9459(6)	15.6585(9)	12.9389(8)	11.700(3)	14.2293(4)
c (Å)	17.0777(8)	26.0358(10)	21.251(1)	32.894(2)	35.766(9)	26.9259(8)
α (deg)	90	90	90	90	90	90
β (deg)	94.735(2)	100.503(2)	107.245(3)	99.185(3)	92.087(3)	92.8940(10)
γ (deg)	90	90	90	90	90	90
V (Å^3)	3749.0(3)	4349.1(3)	9383.5(9)	15520(2)	8409(4)	7265.0(4)
Z	4	4	8	4	8	8
T, K	150(2)	150(2)	150(2)	150(2)	120(1)	150(2)
D_{calcd} (g cm^{-3})	1.590	1.504	1.461	1.367	1.631	1.480
μ (mm^{-1})	0.785	1.259	1.919	0.820	1.935	1.318
min/max transmission	0.8544/0.9648	0.5717/0.7868	0.5038/0.8790	0.7277/0.9284	0.8010/0.9266	0.6427/0.6863
reflection collected	125707	166920	165529	249585	39734	114995
independent reflections [R_{int}]	14315[0.0352]	25918[0.0235]	22776[0.0329]	34195[0.0518]	7755[0.2690]	17609[0.0229]
final R indices [$I > 2\sigma(I)$] R1 (wR2)	0.0249(0.0575)	0.0393(0.0894)	0.0353(0.0957)	0.1396(0.2928)	0.0846(0.2063)	0.0457(0.1148)
final R indices (all data) R1(wR2)	0.0361(0.0625)	0.0475(0.0932)	0.0514(0.1083)	0.1461(0.2954)	0.1739(0.2420)	0.0567(0.1204)

dx.doi.org/10.1021/ic300301d | Inorg. Chem. 2012, 51, 6667−6681

Scheme 1

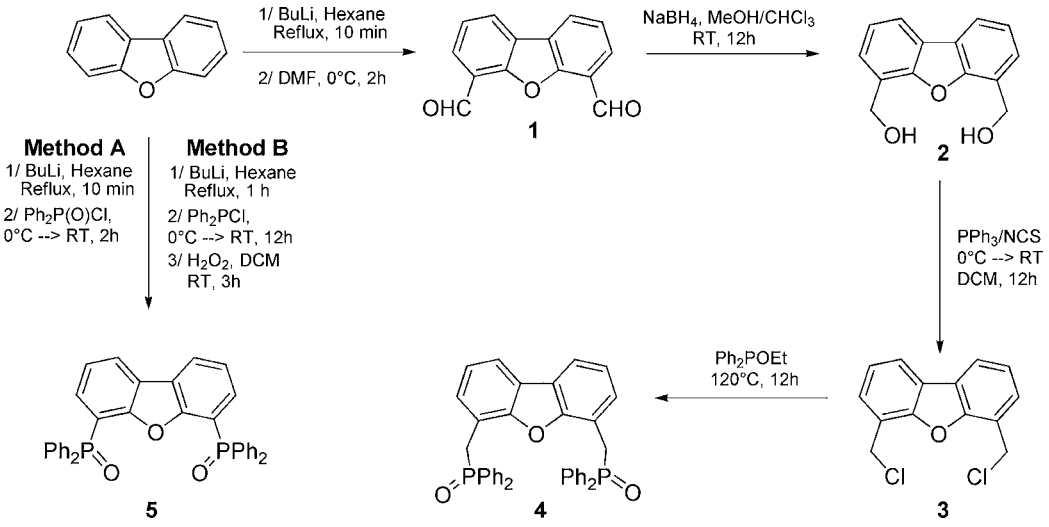

C-atoms were placed in ideal positions with U_{iso} = 1.5U_{eq} of the parent atom. **5**: colorless prisms were grown from MeOH solution of **5** held at −20 °C. *[In(**4**)(NO$_3$)$_3$]*: thin prisms were isolated by slow evaporation of a solution of the complex dissolved in a minimum volume of MeCN/MeOH (20/80) at 23 °C. *[Pr(**4**)(NO$_3$)$_3$(CH$_3$CN)]·0.5CH$_3$CN*: colorless prisms were obtained by slow evaporation (23 °C) of a MeCN/MeOH (90/10) solution of the complex. The H-atoms of the CH$_3$CN molecules were included in ideal positions and refined with fixed U_{iso} = 1.5U_{eq} of the parent C-atom. *[Er(**4**)(NO$_3$)$_3$(CH$_3$CN)]·CH$_3$CN*: thin colorless blades were grown by cooling (−20 °C) a MeCN/MeOH (90/10) solution of the complex. The outer sphere CH$_3$CN is disordered over two positions with occupancies 56.8% (N1s,C1s,C2s) and 43.2% (N2s,C3s,C4s). The H-atoms were included in ideal positions and refined with fixed U_{iso} = 1.5U_{eq} of the parent carbon atom. *[Pu(**4**)Cl$_4$]·(THF)*: Single crystals were obtained from Method 1. The presence of twin components resulted in relatively large esd values associated with the bond lengths and angles. Repeated attempts at structure determinations with different crystals revealed similar or worse twinning, and the low solubility of the compound prevented growth of crystals from other solvent systems suitable for single crystal X-ray diffraction. *[Nd(**4**)$_2$(NO$_3$)$_2$]$_2$(NO$_3$)$_2$·(H$_2$O)·4(CH$_3$OH)*: colorless needles were obtained by slow evaporation (23 °C) of a CH$_3$OH solution of the complex. The crystals were of marginal quality as a result of the presence of a large number of disordered solvent molecules in the crystal lattice. There were no signs of crystal decay during data collection. In an initial refinement model, one water molecule, disordered over two positions with occupancies of 65% (O1w) and 35% (O2w), and four CH$_3$OH molecules, one disordered over two positions with occupancies of 58.7% (O5s,C5s) and 41.3% (O4s,C4s), were included; however, the R-factors were high. Significant improvement of the R-factors was achieved through use of the SQUEEZE procedure.[45] PLATON estimates 171 electrons unaccounted for in the solvent accessible void volume which leads to an estimate of 9.5 CH$_3$OH molecules or 16 water molecules. Except for the molecules mentioned above, the remaining lattice solvent structure was not satisfactorily modeled. All ordered non-hydrogen atoms were refined anisotropically. The H-atoms on the ligand **4** were included in fixed ideal positions with U_{iso} = 1.2U_{eq} of the parent C-atoms. The ordered CH$_3$OH H-atoms were fixed in ideal positions and refined with U_{iso} = 1.5U_{eq}. *{[Er(**5**)$_2$(NO$_3$)$_2$]-(NO$_3$)·4CH$_3$OH}$_{0.5}$*: colorless prisms were obtained by slow evaporation (−20 °C) of a MeCN/MeOH (90/10) solution of the complex. The Er resides on a crystallographic 2-fold axis so that there are two ligands and two nitrate ions coordinated to Er1. The third nitrate is not coordinated, and it is equally disordered over two positions (50%) about an inversion center. There are two outer sphere CH$_3$OH molecules one of which is ordered [O1s, C1s], and it was refined anisotropically. The second is disordered over two positions with occupancies of 65% and 35%.

Distribution Studies. *Materials.* All salts and solvents were reagent grade and were used as received. Extraction experiments were carried out using 1,2-dichloroethane (OmniSolv, EM Science) as the diluent. The aqueous phases were prepared using nitric acid (J. T. Baker, Ultrex II) and europium nitrate (Aldrich, 99.9%). Distilled, deionized water was obtained from a Barnstead Nanopure filter system (resistivity at least 18.2 MΩ-cm) and used to prepare all the aqueous solutions. The radioisotope ^{241}Am was provided by the Radiochemical and Engineering Research Center (REDC) of ORNL. The radiotracer $^{152/154}$Eu was obtained from Isotope Products, Burbank, CA. Both were added as spikes to the aqueous phases in the sample equilibration vials in the extraction experiments.

Methods. Phases at an 1:1 organic to aqueous (O:A) phase ratio were added to 2 mL polypropylene microtubes, which were then capped and mounted by clips on a disk that was rotated in a constant-temperature air box at 25.0 ± 0.5 °C for 1 h. After the contacting period, the tubes were centrifuged for 5 min at 3000 rpm and 25 °C in a Beckman Coulter Allegra 6R temperature-controlled centrifuge. A 250 μL aliquot of each phase was subsampled and counted using a Canberra Analyst pure Ge Gamma counter. Counting times were sufficient to ensure that counting error was a small fraction of the precision of the obtained distribution ratios, considered from a combination of volumetric, replicate, and counting errors to be ±5%. Americium and europium distribution ratios were calculated as the ratio of the volumetric count rates of the ^{241}Am and $^{152/154}$Eu isotopes in each phase at equilibrium.

Molecular Mechanics Calculations. *Method.* Geometry optimizations of the free and metal-bound forms of NOPOPO, **4** and **5** were carried out with the MM3 force field[46] using a points-on-a-sphere metal ion[47] as implemented in PCModel software.[48] Conformational searches to locate the most stable form for each structure were performed using the GMMX algorithm provided with this software. Input files required to repeat these calculations including additional parameters for treating the metal-dependent interactions are available as Supporting Information.

RESULTS AND DISCUSSION

Ligand Syntheses and Characterization. The syntheses of the target ligands **4** and **5**, developed in the present study, are summarized in Scheme 1. The 4,6-diformyl-dibenzofuran, **1**, was prepared essentially as described in the literature[8] although the realized yield of purified compound was typically about half of that previously reported. The syntheses of 4,6-bis-(hydroxymethyl)-dibenzofuran, **2**, and 4,6-bis(chloromethyl)-dibenzofuran, **3**, were accomplished in a manner similar[49] to procedures briefly outlined by Hanton[11] and Cram[16] for preparation

dx.doi.org/10.1021/ic300301d | Inorg. Chem. 2012, 51, 6667−6681

of 4,6-bis(bromomethyl)-dibenzofuran. Both steps are efficient, and **3** was obtained as a yellow powder. Subsequent reflux of **3** with excess Ph_2POEt under nitrogen, without additional solvent, gave a solid mass that, following removal of the excess Ph_2POEt, left 4,6-bis(diphenylphosphinoylmethyl)-dibenzofuran, 4,6-$[Ph_2P(O)CH_2]_2$DBF, **4**, as a white powder.[50] The compound is soluble in $CHCl_3$, CH_2Cl_2, THF, and hot CH_3CN, less soluble in MeOH and insoluble in cold CH_3CN. The HRESI-MS displays a parent ion, $[M+H^+]$, and an infrared spectrum contains a strong absorption at 1191 cm^{-1} that is tentatively assigned to the ν_{PO} stretching frequency based upon assignments made in related phosphine oxide compounds.[24,28] The ^{31}P NMR spectrum shows a single resonance, whose chemical shift, δ 29.8 in $CDCl_3$ and 34.5 in MeOH-d_4, compares favorably with shifts observed for diphenylphosphinoylmethyl-decorated pyridine and pyridine N-oxide compounds,[24,28] and the ^1H and $^{13}C\{^1H\}$ NMR spectra are consistent with the proposed structure. Most notably, the ^1H and $^{13}C\{^1H\}$ resonances for the methylene group in the $-CH_2P(O)Ph_2$ arms appear at δ 3.91 (J_{PH} = 13.5 Hz) and δ 31.8 (J_{CP} = 66.9 Hz), respectively.

The molecular structure of **4** was confirmed by single crystal X-ray diffraction analysis. A view of the molecule is shown in Figure 1 and selected bond lengths are listed in Table 3. The

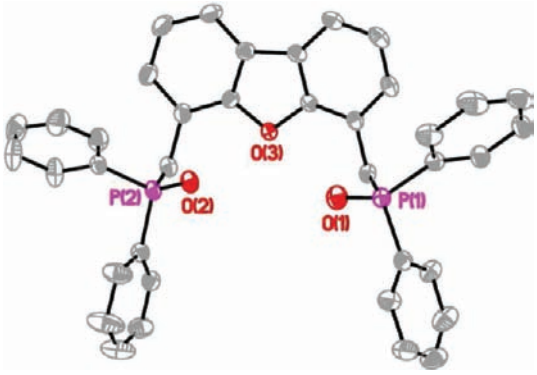

Figure 1. Molecular structure of 4,6-$[Ph_2(O)CH_2]_2$DFB·CH_3OH, **4**·CH_3OH, (thermal ellipsoids, 50%) with lattice CH_3OH omitted for clarity.

Table 3. Selected Bond Lengths for Ligands 4·MeOH and 5 (Å)

bond type	4·MeOH		5	
P–O	P1–O1	1.4934(8)	P1–O2	1.485(1)
	P2–O2	1.4879(8)	P2–O2	1.4857(9)
P–C	P1–C1	1.810(1)	P1–C2	1.812(1)
	P2–C12	1.807(1)	P2–C11	1.804(1)
C–O	C14–O3	1.381(1)	C1–O1	1.385(1)
	C13–O3	1.383(1)	C12–O1	1.385(1)

molecular unit contains a MeOH solvent molecule that is disordered nearly equally over two sites, and it is omitted from the view in Figure 1. The dibenzofuran backbone is planar, and the P═O bond vectors are rotated out of the backbone plane in opposite directions. The P═O bond lengths, P1–O1 1.4934(8) Å and P2–O2 1.4879(8) Å are comparable to the P═O bond length in $[Ph_2P(O)CH_2]_2C_5H_3NO$, 1.480(3) Å.[25] The MeOH solvent molecule is hydrogen bonded with one phosphoryl oxygen atom as indicated by the nonbonded distances, O1S···O1($-x+1$, $-y+1$, $-z+2$), 2.667(11) Å, and O1($-x+1$, $-y+1$, $-z+2$)···H1S, 1.73(9) Å, and the angle, O1S–H1S–O1($-x+1$, $-y+1$, $-z+2$), 166(5)°.

Ligand **5** was prepared in a one-pot synthesis (Method A), as summarized in Scheme 1, by reaction of dibenzofuran with *n*-BuLi/TMEDA solution (1:2) followed by treatment of the putative 4,6-Li_2-DFB with 2 equiv of $Ph_2P(O)Cl$. This approach was initially chosen over an alternative route that would utilize oxidation of the known precursor diphosphine,[1,2] 4,6-$[Ph_2P]_2$-DFB, **6**, since mixed substituent derivatives, 4,6-$[RR'P(O)CH_2]_2$-DFB, of potential interest for extraction measurements might be reached efficiently by using more easily prepared alkyl and aryl phosphinic chlorides than with the mixed substituent phosphines. Surprisingly, this direct approach, proved to be somewhat inefficient as indicated by the low, unoptimized yield (18%) of **5**. Synthetic variations that might provide improved yields have not yet been explored. The modest yield encountered with Method A led us to prepare **5** via oxidation of the known phosphine, **6**, (Method B), and the yield of **5** improved (50%). Compound **5** displays a parent ion, $[M+H^+]$ in the HRESI-MS, and the IR spectrum contains a strong absorption at 1181 cm^{-1} tentatively assigned to a P═O stretching mode. The ^{31}P NMR spectrum has a single resonance, δ 25.2, and the ^1H and $^{13}C\{^1H\}$ NMR spectra are consistent with the proposed structure. The molecular structure of **5** was further confirmed by single crystal X-ray diffraction analysis, and a view of the molecule and selected bond lengths are presented in Figure 2 and Table 3, respectively.

Figure 2. Molecular structure of 4,6-$[Ph_2(O)]_2$DFB, **5**, (thermal ellipsoids, 50%).

The dibenzofuran backbone is planar with the two P═O bond vectors twisted out of the plane by different amounts as indicated by the dihedral angles, O2–P1–C2–C1 −54.9(1)° and O3–P2–C11–C10 4.4(1)°. The P═O bond lengths, P1–O2, 1.4849(10) Å and, P2–O3, 1.4857(9) Å are identical and comparable with the bond lengths in **4**·MeOH. It is noted that during the course of this study a report of the synthesis of **5** by hydrogen peroxide oxidation of **6** appeared along with a crystal structure determination,[15] but parametric data are absent in the report, and apparently the X-ray diffraction data have not yet been deposited.

As noted in the Introduction, a synthesis for the diphosphine, 4,6-$(Ph_2P)_2$DBF, **6**, has been previously reported,[1,2] and options for bidentate PP′ vs tridentate POP′ chelation on transition metal centers have been evaluated. The rigid character of the backbone, the large separation of the P-atom donor centers (5.741 Å), and the calculated bite angle range (117–147°) suggested that this diphosphine would prefer to form bimetallic complexes. Indeed, coordination of **6** to a $Co_2(CO)_6$ fragment

dx.doi.org/10.1021/ic300301d | Inorg. Chem. 2012, 51, 6667–6681

gave a bimetallic complex, $Co_2(CO)_6$(**6**), in which the ligand bridges the two Co(0) atoms, and the furan O-atom is not involved in the ligand/metal interaction.[3] However, subsequent coordination chemistry with Ru(III) revealed complexes containing tridentate POP′ chelate interactions.[10] To adopt this structure the nonbonded P···P separation decreased by ∼1 Å, and the bite angle increased by ∼25° relative to the free ligand. Molecular modeling suggested that this deformation results in steric strain in excess of 3 kcal/mol.[4] The reaction of **6** with $Re_2Cl_8^{2-}$ also produced a complex with a tridentate POP′ chelate interaction on one of the Re centers and a monodentate P interaction on the other.[10] Given these observations, it was of interest to explore the coordination preferences for both the bis(methylphosphine oxide), **4**, and the more rigid bis(phosphine oxide), **5**.

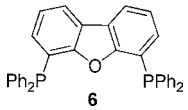

6

Ligand Computational Modeling. Qualitative CPK model building suggests that both of the bis(phosphine oxide)-type ligands, **4** and **5**, should, at the least, be able to act as bidentate, POP′O′ chelating ligands on trivalent or tetravalent *f*-block element cations. However, it is not clear if the furan O-atom can join with these donor centers to form tridentate chelate structures without incurring serious ligand strain. Therefore, computational molecular mechanics (MM) assessments of the ligand strain energies developed during the transformation of the ligands from their free, unbound resting states to metal bound bidentate (PO donors only) and tridentate (both PO and O_{furan} donors) chelate structures were undertaken to address this issue.[51] Such strain energies, which can be evaluated in the absence of other factors such as auxiliary inner-sphere ligation or outer-sphere solvation, provide a quantitative measure of the intrinsic ability of the ligand to achieve the bound conformation. When evaluated in the tridentate bonding mode with Pr(III), the computed strains developed in **4** and **5**, relative to their free ligand conformations, are 13.8 and 11.9 kcal/mol, respectively. These results indicate that both **4** and **5** are structurally less organized for tridentate metal coordination than NOPOPO, which exhibits a corresponding ligand strain of only 8.8 kcal/mol. Bidentate chelation interactions by **4** and **5** result in less ligand strain than tridentate chelation. However, with strain energies of 9.3 kcal/mol, **4**, and 9.0 kcal/mol, **5**, these ligands are still more strained than tridentate NOPOPO. Views of the computed energy-minimized tridentate metal complexes are shown in Figure 3.

The computed ligand strain energies reflect the degree of binding site organization provided by these scaffolds.[51] An important component to this organization is how well the spatial arrangement of donor groups in the binding conformation is able to complement the metal ion. As illustrated in an earlier review on the role of donor atom orientation in metal ion binding,[52] a convenient device for visualizing the degree of complementarity offered by a ligand binding conformer is to add vectors to each donor atom that represent the direction for optimal metal interaction with the donor atom. When all vectors converge at the correct M−L distance, the ligand is complementary. The orientation of these vectors, which reflect optimal M−L−X angles and M−L−X−X dihedral angles, can be deduced from crystal structure data for complexes involving simple monodentate ligands.

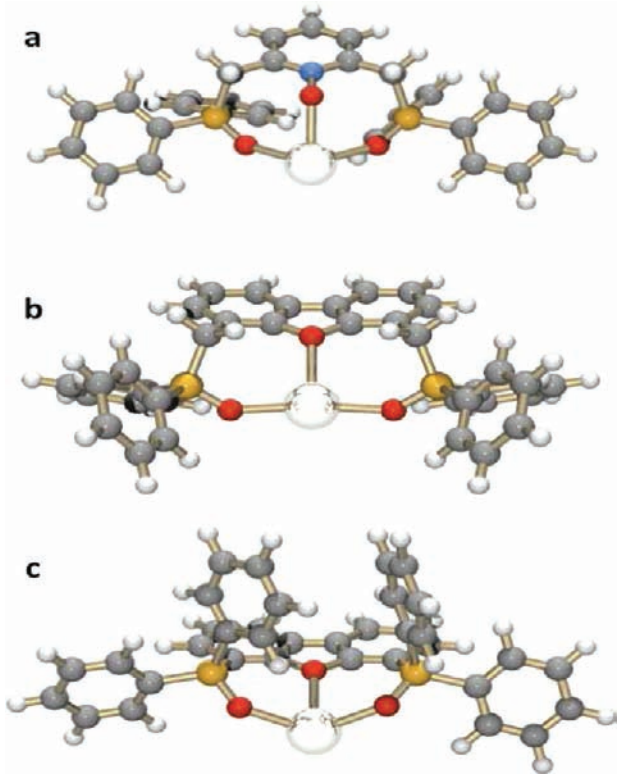

Figure 3. Geometry optimized structures for tridentate coordination in 1:1 ligand Pr(III) complexes: (a) NOPOPO, (b) ligand **4**, and (c) ligand **5**.

A search of the Cambridge Structural Database[53] for crystal structures involving *f*-element cations coordinated to monodentate triaryl phosphine oxides, pyridine-N-oxides, and ethers was conducted. As shown in Figure 4a, phosphine oxide interactions exhibit an average P═O−M bond angle of 163 ± 10° with no clear preference for C−P═O−M dihedral angles. As illustrated in Figure 4b, pyridine-N-oxide interactions display N−O−M angles of 132 ± 8° and dihedral angles covering a wide range, 90 ± 33°. Finally, as indicated in Figure 4c, ether interactions exhibit C−O−M angles in a more narrow range, 125 ± 4°, with an out-of-plane angle, 0 ± 8°, consistent with prior observations that the ether oxygen donor atom prefers sp^2 hybridization.[52]

As shown in Figure 5, these data can be used to visualize the donor orientation provided by the binding conformers of NOPOPO, **4**, and **5**. The resulting picture is consistent with the ligand strain analysis results. NOPOPO, which develops the least amount of strain upon metal complexation, exhibits the most convergent set of vectors, that is, this scaffold allows all three donor-metal interactions to achieve geometries closest to those observed for monodentate analogues. In both **4** and **5**, the architectures position the two P═O donors to simultaneously coordinate the metal, but fail to correctly orient the ether oxygen donor group. The degree of vector convergence is better in **5** than in **4**, which exhibits the largest strain on metal coordination. Thus, both ligand strain analysis and evaluation of donor orientation predict that, of these three ligands, **4** is least likely to engage in tridentate coordination.

Coordination Chemistry. With these results in mind, the coordination chemistry of **4** was initially explored with several small, trivalent *p*-block metal cations, Al(III), Ga(III), and In(III), as their nitrate salts, with ligand:metal combining ratios

dx.doi.org/10.1021/ic300301d | *Inorg. Chem.* 2012, 51, 6667−6681

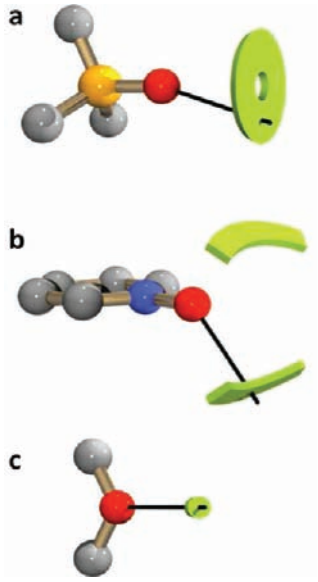

Figure 4. Depiction of the observed location of *f*-block metal ions coordinated with monodentate (a) triaryl phosphine oxides, (b) pyridine N-oxides, and (c) ethers in the Cambridge Structural Database.[51] Observed metal locations are illustrated by green volumes, and the black vector emanating from each oxygen atom represents an average direction of approach for the metal ion.

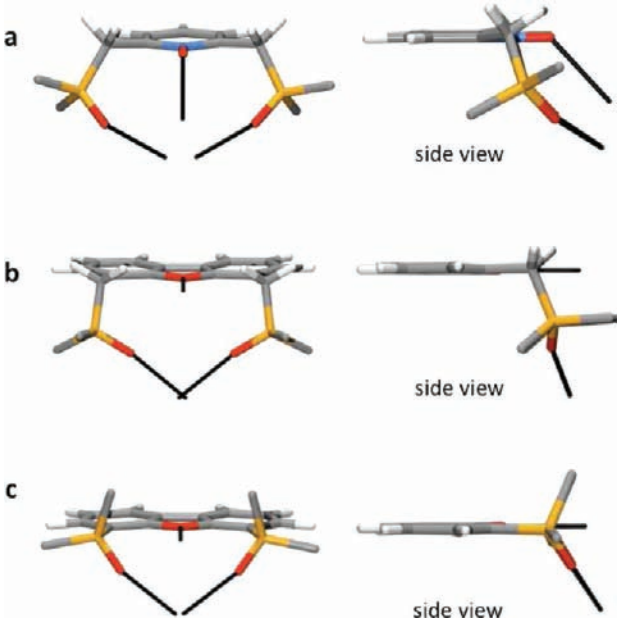

Figure 5. Donor group orientation in the binding conformation of (a) NOPOPO, (b) ligand **4**, and (c) ligand **5** illustrated with 2.5 Å vectors emanating from each donor oxygen atom in the optimal direction for metal binding (see Figure 4). P-phenyl groups are replaced with carbon atoms for clarity.

of 1:1 and 2:1. Under the conditions explored, the CH elemental analyses suggest that in each case these *p*-block metal cations form mixtures that contain both 1:1 and 2:1 complexes.[50] The IR spectra for the complexes display a strong band tentatively assigned to the P═O stretching mode with a coordination shift, $\Delta\nu_{PO}$ ~50 cm^{-1}, relative to the free ligand. This coordination shift is consistent with metal−ligand binding at least through one or both phosphine oxide donor groups. There is also a new absorption at ~1200 cm^{-1}($\Delta\nu$ ~+10 cm^{-1}) that may arise from an unbound P═O group in a monodentate **4**. The ^{31}P NMR spectrum for a 1:1 mixture of **4** and $In(NO_3)_3$ dissolved in MeOH-d_4 shows a single resonance, δ 35.1, that is only slightly shifted from the free ligand in MeOH-d_4, δ 34.5. A 2:1 mixture and a 4:1 mixture show a single resonance at δ 35.4 and 34.7, respectively, indicating that the ligand is undergoing rapid exchange on the In(III) in methanol solution. Crystallization of a crude sample of the indium(III) complex, obtained from the 1:1 combination of **4** and $In(NO_3)_3$, from a mixed MeCN/MeOH solvent mixture, provided single crystals for which a single crystal X-ray structure determination reveals the composition [In(**4**)$(NO_3)_3$]. A view of the complex is shown in Figure 6, and selected bond lengths are listed in Table 4. The

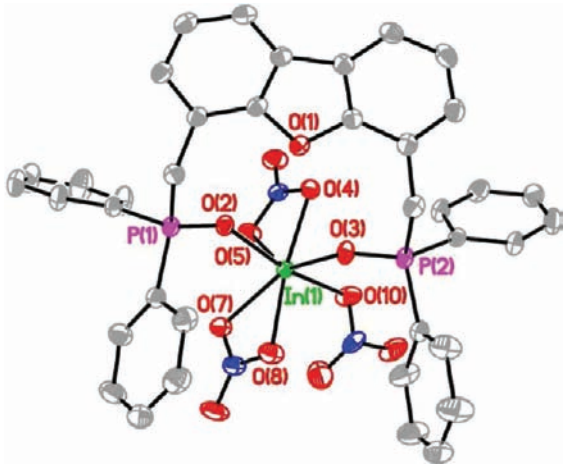

Figure 6. Molecular structure and atom labeling scheme for [In(**4**)$(NO_3)_3$] (thermal ellipsoids, 50%) with H-atoms omitted for clarity.

In(III) ion displays a seven coordinate pentagonal bipyramidal inner coordination sphere generated by two oxygen atoms from the P═O groups of a bidentate ligand **4**, four oxygen atoms from two bidentate nitrate ions, and one O-atom from a monodentate nitrate ion. A similar bidentate/monodentate nitrate coordination condition on In(III) was observed in the complex [In$(bipy)_2(NO_3)_3$] in which the bipyridyl ligands are both bidentate, one nitrate ion is bidentate and two nitrate ions are monodentate.[54] The furan O-atom is 4.209 Å removed from the In(III), and the nonbonded In1···O3 vector is 22.3° out of the DBF_{ring} plane. These features are consistent with the absence of a coordinate bond interaction between the indium ion and the DBF O-atom. The average In−O(P) bond length, 2.0967 ± 0.0002 Å, is relatively short compared to bond lengths in several phosphine oxide complexes of indium halides: [In$(Ph_3P(O))_2(Br)_2(CH_2Br)$], 2.281(6) Å (avg)[55] and [In$(Me_2PhP(O))_2Cl_3$], 2.196(7) Å (avg).[56] The average P═O bond length in the coordinated ligand, 1.5108 ± 0.0004 Å, is elongated relative to the average P═O bond length in the free ligand, 1.4907 ± 0.0028 Å. Attempts to isolate and structurally characterize 2:1 complexes of these Group 13 cations that might contain **4** binding with both bidentate and monodentate coordination modes have so far been unsuccessful. However, the fact that the nitrate ions show mixed coordination modes in the [In(**4**)$(NO_3)_3$] solid state structure support the suggestion that 2:1 complexes may contain mixed ligand binding

dx.doi.org/10.1021/ic300301d | *Inorg. Chem.* 2012, 51, 6667−6681

Table 4. Selected Bond Lengths for Coordination Complexes (Å)

bond type	[In(**4**)$(NO_3)_3$]		[Pr(**4**)$(NO_3)_3(CH_3CN)$]·0.5(CH_3CN)		[Er(**4**)$(NO_3)_3(CH_3CN)$]·(CH_3CN)		[Nd(**4**)$_2(NO_3)_2]_2(NO_3)_2$·(H_2O)·4(CH_3OH)		[Pu(**4**)Cl_4]·(THF)		{[Er(**5**)$_2(NO_3)_2$]-(NO_3)·2$CH_3OH\}_{0.5}$	
M−O(P)	In1−O2	2.0965(9)	Pr1−O1	2.333(1)	Er1−O2	2.240(2)	Nd1−O2	2.363(7)	Pu1−O1	2.207(11)	Er1−O2	2.243(1)
	In1−O3	2.0969(9)	Pr1−O2	2.367(1)	Er1−O3	2.248(2)	Nd1−O3	2.374(7)	Pu1−O2	2.246(11)	Er1−O3	2.254(2)
							Nd1−O5	2.382(7)			Er1−O4	2.432(2)
							Nd1−O6	2.358(8)			Er1−O6	2.453(2)
M−Cl									Pu1−Cl1	2.552(5)		
									Pu1−Cl2	2.560(5)		
									Pu1−Cl3	2.568(4)		
									Pu1−Cl4	2.577(7)		
M−O(nitrate)	In1−O10	2.150(1)	Pr1−O7	2.511(1)	Er1−O5	2.398(2)	Nd1−O7	2.525(8)			Er1−O4	2.432(2)
	In1−O8	2.252(1)	Pr1−O4	2.515(1)	Er1−O7	2.408(2)	Nd1−O8	2.543(8)			Er1−O6	2.453(2)
	In1−O7	2.270(1)	Pr1−O5	2.554(1)	Er1−O4	2.408(2)	Nd1−O10	2.520(7)				
	In1−O4	2.284(1)	Pr1−O10	2.563(2)	Er1−O10	2.448(2)	Nd1−O11	2.488(8)				
	In1−O5	2.291(1)	Pr1−O11	2.573(2)	Er1−O8	2.465(2)						
			Pr1−O8	2.581(2)	Er1−O11	2.507(2)						
avg	In−O(bidentate avg)	2.274	Pr−O (avg)	2.550	Er−O(avg)	2.439					Er−O(avg)	2.443
M−N(solvent)			Pr1−N4	2.622(2)	Er1−N4	2.447(3)						
P−O	P1−O2	1.5111(9)	P1−O1	1.502(1)	P1−O2	1.5009(2)	P1−O2	1.506(7)	P1−O1	1.511(11)	P1−O2	1.499(2)
	P2−O3	1.5104(9)	P2−O2	1.497(1)	P2−O3	1.496(2)	P2−O3	1.507(8)	P2−O2	1.515(11)	P2−O3	1.504(2)
							P3−O5	1.488(7)				
							P4−O6	1.502(8)				

dx.doi.org/10.1021/ic300301d | Inorg. Chem. 2012, 51, 6667−6681

conditions with one or more nitrate counter-ions displaced to the outer coordination sphere.

The coordination chemistry of **4** with the lanthanide cations La(III), Pr(III), Nd(III), Eu(III), and Er(III), all as their nitrate salts, was examined by using 1:1 and 2:1 ligand:metal combining ratios in MeOH/EtOAc (1:1) solvent. Under the conditions explored, the 1:1 complexes, like the free ligand, are very soluble in CH_2Cl_2 and $CHCl_3$, while in MeOH, MeCN, and DMF solubility is reduced. The complexes obtained from 2:1 combinations are also soluble in CH_2Cl_2 and $CHCl_3$, but the solubility in the other solvents is much lower than for the complexes isolated from 1:1 combinations. Each complex was obtained as a solid powder following evaporation of solvent. Attempts were made to deduce the precise compositions of the complexes by elemental analyses prior to mixed-solvent recrystallizations that produced the single crystal samples used for X-ray diffraction analyses. Satisfactory agreements were obtained for complexes formulated as $[La(\mathbf{4})(NO_3)_3]\cdot H_2O$, $[Pr(\mathbf{4})(NO_3)_3]\cdot H_2O$, and $[Nd(\mathbf{4})_2(NO_3)_3]\cdot$MeOH. The analyses for the remaining samples suggested formation of mixtures of 1:1 and 2:1 complexes. For single crystal samples, the agreements between measured and calculated CH compositions, based upon the crystallographically determined compositions, were not within ±0.4%. This is due, in part, to the presence of loosely held lattice solvent molecules. High resolution mass spectra for selected samples were also collected; however, parent ions were not observed. This suggests that the complexes do not survive the ionization conditions of the ESI-MS spectrometer employed. The IR spectra for the samples with 1:1 and 2:1 compositions are essentially identical with all showing significant $\Delta\nu_{PO}$ shifts in the range 49−52 cm^{-1}. The ^{31}P NMR spectrum for the 1:1 complex $[La(\mathbf{4})(NO_3)_3]$ in MeOH-d_4 shows a single resonance, δ 35.6, shifted ∼1 ppm from the free ligand. Further additions of **4** to the solution resulting in 2:1 and 4:1 ligand:La(III) reactant ratios gave spectra with a single resonance, δ 35.2, consistent with rapid ligand exchange. Attempts were also made to study the complexation of **4** with La(III) in aqueous solution by using spectrophotometric-based metal titrations, but low binding energy (log K_1 ∼ 0.2) hindered this analysis. As a result, single crystal X-ray diffraction analyses provide the most definitive composition and structural characterization for the crystalline complexes.

The inner sphere structures for the 1:1 complexes $[Pr(\mathbf{4})(NO_3)_3(CH_3CN)]\cdot 0.5CH_3CN$ and $[Er(\mathbf{4})(NO_3)_3(CH_3CN)]\cdot CH_3CN$ are shown in Figures 7 and 8, respectively, and selected bond lengths are summarized in Table 4. The inner sphere structures are identical except for small differences in the Ln-O and Ln-N distances because of variations in lanthanide ionic radii and the greater polarizing strength of Er(III). The structures contain a bidentate POP′O′-bonded ligand **4**, three bidentate nitrate groups and one N-bonded acetonitrile molecule. The eight oxygen atoms and one nitrogen atom, in both cases, produce a tricapped trigonal prismatic coordination polyhedron. The bidentate chelate interaction in the Pr(III) complex is slightly asymmetric, Pr1−O1 2.333(1) Å and 2.367(1) Å, while the interaction is more symmetric in the Er(III) complex, Er1−O2 2.240(2) Å and 2.248(2) Å. The DBF ring, including the O-atom, is planar but not O-bonded to the Ln ions; the nonbonded $Ln\cdots O_{DBF}$ separations are 4.280 (Pr) and 4.265 Å (Er), respectively, and the nonbonded $M\cdots O_{furan}$ vectors make an angle of 18° with the DBF plane. The Ln-O(P) bond lengths are similar to those found in Pr(III) and Er(III) complexes containing alkyl decorated POP′O′NO″ ligands[31] and slightly shorter than

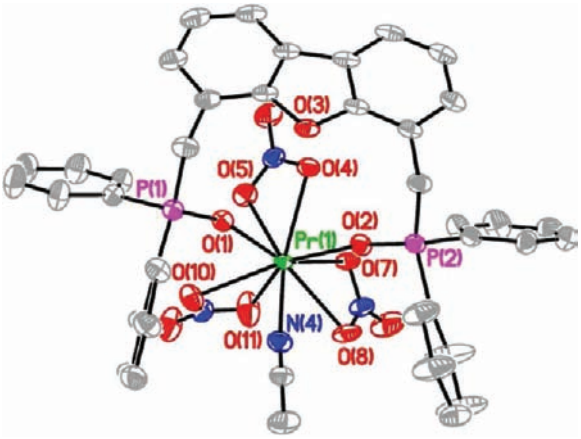

Figure 7. Molecular structure and atom labeling scheme for $[Pr(\mathbf{4})(NO_3)_3(CH_3CN)]\cdot 0.5CH_3CN$ (thermal ellipsoids, 50%) with lattice CH_3CN and H-atoms omitted for clarity.

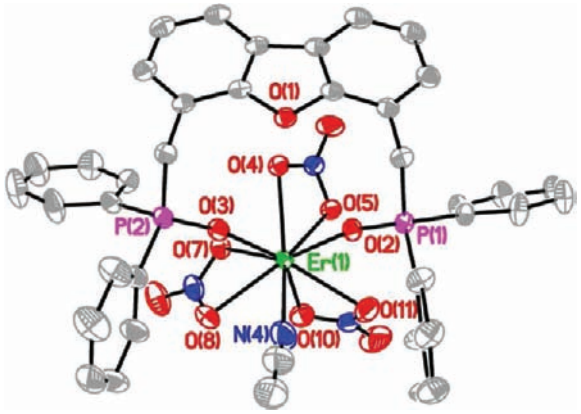

Figure 8. Molecular structure and atom labeling scheme for $[Er(\mathbf{4})(NO_3)_3(CH_3CN)]\cdot CH_3CN$ (thermal ellipsoids, 50%) with lattice CH_3CN and H-atoms omitted for clarity.

found with the phenyl substituted POP′O′NO″.[24,28] The P═O bond lengths are slightly elongated over the values observed in the free ligands.

Considerable effort was devoted to isolation of X-ray quality single crystals of 2:1 complexes containing **4**. Unfortunately, in all cases, crystal quality was poor as a result of the presence of disordered solvent molecules that could not be adequately modeled. The refinement for one complex, $\{[Nd(\mathbf{4})_2(NO_3)_2](NO_3)\cdot(H_2O)\cdot 4(CH_3OH)\}_{0.5}$, following application of SQUEEZE to obtain a solvent free structure, is presented since the qualitative structural features are worth noting. A view of the inner sphere structure is shown in Figure 9. The structure contains two ligands, **4**, and both are bonded in a POP′O′ bidentate mode. The DBF O-atoms are well removed from the Nd(III) at 4.22 and 4.20 Å. This result indicates that there is sufficient space to accommodate two bidentate POP′O′ coordinated molecules of **4** in the Nd(III) inner coordination sphere, but additional structural conclusions should not be drawn given the crystal quality.

The coordination chemistry of **4** toward Pu(IV) was also explored. Initially it was noted that addition of aqueous Pu(IV)/HCl solution to a MeOH solution of **4** produced a yellow precipitate, as did addition of Pu(IV)/HCl solution to **4** in hot CH_3CN. These precipitates, assumed to be a Pu(IV) complex with **4**, did not redissolve in CH_2Cl_2 or hot MeOH.

dx.doi.org/10.1021/ic300301d | Inorg. Chem. 2012, 51, 6667−6681

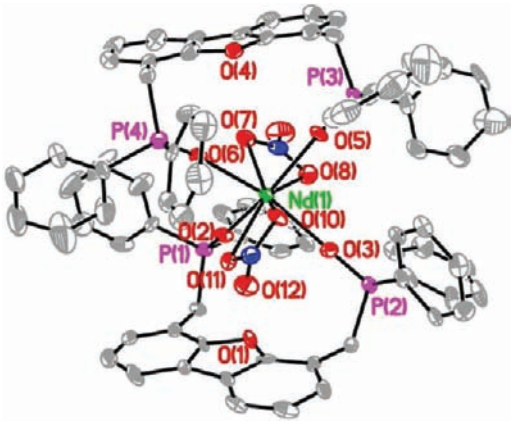

Figure 9. Molecular structure and atom labeling scheme for $[Nd(\mathbf{4})_2(NO_3)_2^+](NO_3^-)\cdot(H_2O)\cdot 4(CH_3OH)$ with outer sphere nitrate ion, lattice solvent molecules, and H-atom omitted for clarity (thermal ellipsoids, 30%).

Therefore, the complexation of Pu(IV) with **4** was followed by visible/near-IR spectrometry in THF solution. As shown in Figure 10, the spectra of aliquots of the initial yellow Pu(IV)

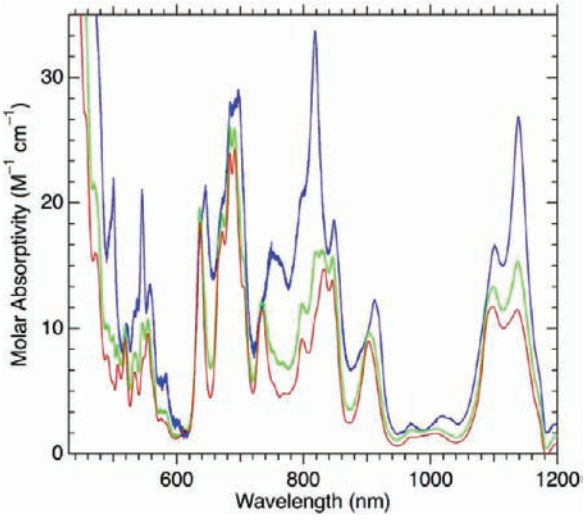

Figure 10. Solution electronic absorption spectra of various concentrations of aqueous Pu(IV)/HCl in THF. The Pu(IV) concentrations are 2.0 mM (blue), 5.9 mM (green), and 22.7 mM (red).

hydrochloric acid stock solution, spiked into THF, differ depending on the concentration of the Pu(IV)/HCl in THF, but they resemble the spectra of $[PuCl_6]^{2-}$ in CH_3CN[57] (green trace). This suggests that the $[PuCl_6]^{2-}$ anion may not be the only species present in THF solution prior to addition of **4** (e.g., other plutonium chloride or solvation species).[58] However, the differences in the initial spectra do not affect the form of the spectra once **4** is added. Figure 11 shows the vis–NIR spectra as increasing equivalents of **4** are added to the Pu(IV)/HCl solution in THF solvent. Visually, the original distinct yellow color becomes less intense with each addition. The electronic transitions for actinide ions are generally broader and more sensitive to the local ligand environment than the more "core-like" lanthanide ions, allowing changes in the profiles of the 5f-5f and 5f-6d transitions to be a useful tool in following speciation changes of actinide ions. The formation of a Pu(IV) complex is

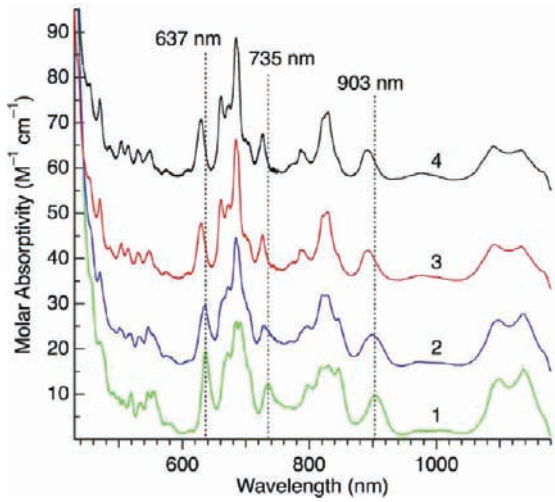

Figure 11. Solution electronic absorption spectrum of 2–6 mM Pu(IV) in THF as a function of added **4**. Equivalents of added **4**: 0 (1), 0.44 (2), 0.88 (3), 1.77 (4). For legibility, spectra 2, 3, and 4 have been offset on the *y*-axis by 15, 34, and 55 M^{-1} cm^{-1}, respectively.

evident by blue shifts in the transitions at 637, 735, and 903 nm to 630, 727, and 892 nm, respectively. In addition, there are marked profile changes in the electronic transitions in the regions of 650–720 and 780–870 nm, with new maxima appearing at 661 and 786 nm. From the spectra in Figure 11 it appears that only one Pu(IV) complex is formed with **4**. The spectra of 0.88, 1.77, and 3.6 equiv of ligand added are essentially identical, consistent with the assignment of a 1:1 Pu(IV):**4** complex stoichiometry as the only product. This complex is readily precipitated from THF solution as a powder in 66% yield. However, once isolated, the complex exhibits poor solubility in a wide range of organic solvents tested. To obtain NMR spectra, samples of the complex were prepared in situ by mixing Pu(IV)/HCl with 1.1 equiv of **4** in THF-d_8 solution. The ^{31}P NMR spectrum exhibits a paramagnetically broadened resonance at 0.58 ppm, which is assigned to the 1:1 Pu(IV):**4** complex. This resonance is significantly shifted from the sharp "free" ligand resonance at 24.2 ppm (THF-d_8) or 29.8 ppm ($CDCl_3$). The ^1H NMR spectrum is more complicated because of paramagnetic line broadening induced by the proximity of the Pu(IV) ion ($5f^4$ electronic configuration) and the presence of a large resonance at 4.79 ppm due to the protons from the Pu(IV)/HCl solution used in the sample preparation. However, by using the free ligand ^1H NMR spectrum in THF-d_8 as a guide, along with integral values from the in situ spectrum of the $[Pu(\mathbf{4})Cl_4]$ complex, tentative assignments can be made. The peaks at 8.10, 7.00, and 6.32 ppm are in the expected aryl region. All three have equivalent integration values, and can be assigned to the *ortho*-, *meta*-, and *para*-protons on the benzo rings of the DBF backbone, but we cannot say which peaks correspond to H_o, H_m, or H_p positions. The combined integrations of the peaks at 7.59 and 7.40 ppm sum to a value nine times as large as each of the 8.10, 7.00, and 6.32 ppm peaks. Therefore these two peaks likely account for overlapping *ortho*, *meta*, and *para* protons on the phenyl rings (although the integration of these two peaks should be ten times as great instead of nine to accurately account for all of the protons on the phenyl rings). Finally, the alkyl CH_2 protons, which appear as a doublet (due to ^{31}P coupling) at about 4.1 ppm in the THF-d_8 free ligand spectrum, are either too proximate to the paramagnetic Pu(IV) ion to be observed because of line

dx.doi.org/10.1021/ic300301d | Inorg. Chem. 2012, 51, 6667–6681

broadening or they are masked by the large resonance of excess protons arising from the Pu(IV)/HCl solution aliquot. The solid-state vis−NIR diffuse reflectance spectrum of the isolated Pu(IV) complex with **4** is shown in Figure 12 (blue trace). It shows

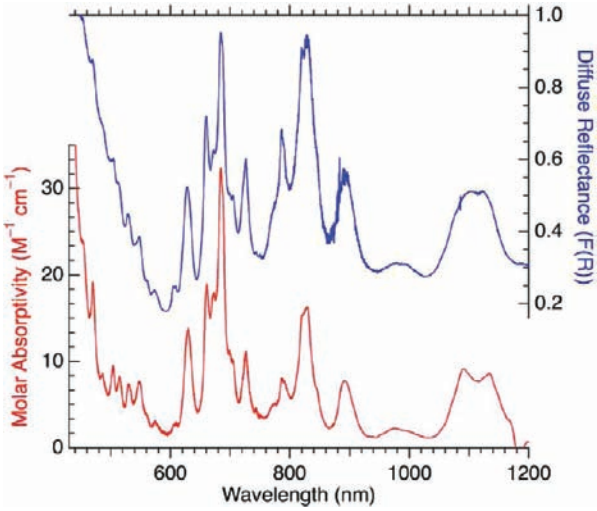

Figure 12. vis−NIR diffuse reflectance spectrum of solid [Pu(**4**)Cl_4] (blue spectrum, right axis). The solution electronic absorption spectrum of 3.5 mM Pu(IV) in THF with 0.88 equiv added **4** (red spectrum, left axis).

excellent correlation of the electronic transitions compared to the solution spectra (Figure 12, red trace), supporting a conclusion of identical speciation in both solid and solution phases.

Confirmation of the 1:1 Pu(IV):**4** stoichiometry is provided by a structure determination on an X-ray diffraction quality single-crystal obtained by slow evaporation of a THF/MeOH solution of the complex. A view of the molecular structure is shown in Figure 13, and pertinent bond distances are provided

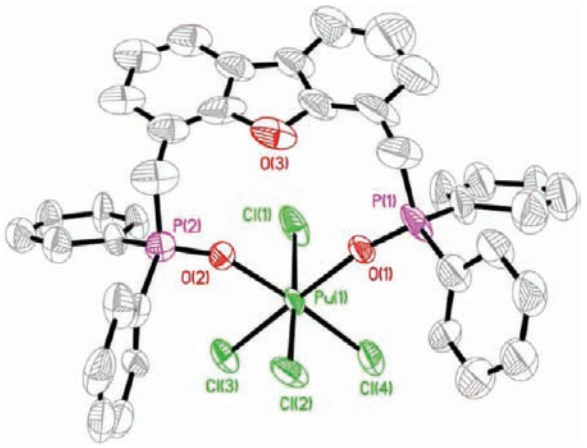

Figure 13. Molecular structure and atom labeling scheme for [Pu(**4**)Cl_4]·THF (50% thermal ellipsoids) with lattice THF and all H-atoms omitted for clarity.

in Table 4. The Pu(IV) ion is six coordinate, bound to four chloride anions and two oxygen atoms from the bidentate ligand, **4**. The geometry about the Pu(IV) ion is best described as distorted octahedral with the O atoms bound in a *cis* arrangement enforced by the requirements of the DBF backbone. The DBF oxygen atom is not coordinated, and it

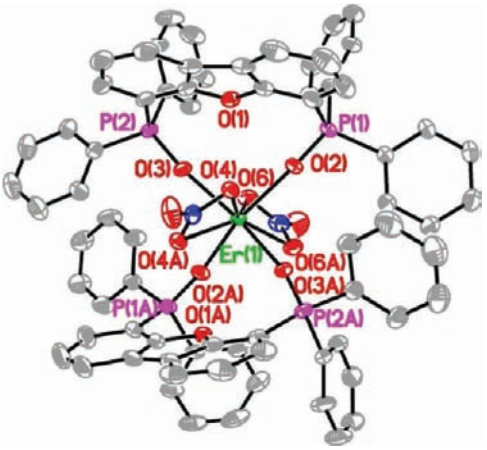

Figure 14. Molecular structure and atom labeling scheme for [Er(**5**)$_2$-$(NO_3)_2$](NO_3)·$2CH_3OH$ (50% thermal ellipsoids) with H atoms, outer sphere nitrate and lattice solvent omitted for clarity.

sits at over 4.2 Å away from the Pu(IV) ion. The Pu−O bond distances to the phosphine oxide O-atoms are 2.207(11) and 2.227(16) Å, while the Pu−Cl distances range from 2.552(5) to 2.577(7) Å. The closest geometrical and chemical comparison in the literature is the *cis*-[$PuCl_4(Ph_3PO)_2$] complex,[59] in which the triphenylphosphine oxide Pu−O distance is 2.221(4) Å, and the Pu−Cl distances are 2.570(2) and 2.572(2) Å. Both are statistically identical to the corresponding bond lengths in [Pu(**4**)Cl_4]. The bite angle, O−Pu−O, for **4** in [Pu(**4**)Cl_4] is 94.2(4)°,which is larger than the O−Pu−O angle of 89.2(2)° in [$PuCl_4(Ph_3PO)_2$]. This difference probably results from the geometric constraints imposed by the DBF backbone compared to the relative freedom of the two unattached Ph_3PO ligands in [$PuCl_4(Ph_3PO)_2$]. Additional related examples of Pu(IV)/phosphine oxide complexes with aromatic ligand backbones have been described.[26,29,60] For example, a ten-coordinate Pu(IV) complex, [$Pu(NO_3)_2$(NOPOP′O′)$_2$]$(NO_3)_2$·$1.5H_2O$·0.5 MeOH (NOPOP′O′ = 2,6-[$(C_6H_5)_2P(O)CH_2]_2C_5H_3NO$), contains two NOPOP′O′ ligands bonded in a tridentate mode through the two P═O and one N−O functionalities.[26] The average Pu−O(P) distance, 2.347 Å, is over 0.1 Å longer than the bond lengths in [Pu(**4**)Cl_4]. This is likely a reflection of the larger coordination number and increased steric congestion in the 1:2 complex. In another ten coordinate 1:2 complex, [$Pu(NOPO)_2(NO_3)_3$][$Pu(NO_3)_6]_{0.5}$, the related bifunctional NOPO ligand, (2-[$(C_6H_5)_2P(O)CH_2]C_5H_4NO$), adopts a bidentate chelate bonding mode in which the Pu−O(P) distances are also over 0.1 Å longer than in [Pu(**4**)Cl_4]. Finally, structures for two 1:1 Pu(IV):POPO complexes (POPO = 2,6-[$(C_6H_5)_2P(O)CH_2]_2C_6H_4$) have been reported.[29] In an eight coordinate [Pu(POPO)$(NO_3)_2Cl_2$] complex, the Pu−O(P) bond distances are similar to those in [Pu(**4**)Cl_4], while in a nine coordinate complex, [Pu(POPO)$(NO_3)_3$(OMe)], the Pu−O(P) bond lengths are slightly longer at 2.301(2) and 2.276(2) Å.

Clearly, the solid-state structural results, regarding the denticity of **4** when bound with hard trivalent and tetravalent metal ions, are consistent with the molecular modeling analysis. It is worth noting that the nonbonded M···O_{furan} distances in the structurally similar 1:1 complexes of **4** are comparable, M = Pr^{3+} (4.280 Å), Er^{3+} (4.263 Å), Pu^{4+} (4.292 Å), and In^{3+} (4.209 Å), but the differences do not directly parallel the differences in metal crystal radii:[61] Pr^{3+} (1.28 Å, CN = 8), Er^{3+} (1.14 Å, CN = 8), Pu^{4+} (1.00 Å, CN = 6), and In^{3+} (1.063 Å, CN = 8). The differences

dx.doi.org/10.1021/ic300301d | *Inorg. Chem.* 2012, 51, 6667−6681

may more reflect the residual effective polarizing strengths of the respective metal cation−anion units and their respective impacts on the framework structure of **4**. Some support for this conclusions is found in the two nonbonded Nd···O_{furan} distances in the 2:1 complex $[Nd(\mathbf{4})_2(NO_3)_2]_2(NO_3)_2$ (4.221 and 4.204 Å). Here, despite expected steric crowding because of the proximity of two large bidentate ligands in the inner coordination sphere, both O_{furan} atoms are drawn closer to the $Nd(NO_3)_2^+$ unit than is the case with the 1:1 complexes containing $Ln(NO_3)_3$ units.

In any case, it is apparent that the anticipated weak M-O_{DBF} bond strength and the stabilization that might be gained through tridentate POP′O′O″-metal interaction are not sufficient to offset the added strain energy incurred in forming the 1:1 or 2:1 complexes with tridentate **4**.

Recalling that the computational modeling analyses suggested that the ligand strain energy for tridentate binding of **5** was less than with **4**, the coordination chemistry of **5** with Pr(III), Eu(III) and Er(III) nitrates, using 1:1 and 2:1 combining ratios, was also explored. In each case, complexes form; however, diffraction quality single crystals of only one complex, $\{[Er(\mathbf{5})_2(NO_3)_2^+](NO_3^-)\cdot 4(CH_3OH)\}_{0.5}$, have so far been obtained. A view of the molecule is shown in Figure 14 and selected bond lengths are presented in Table 4. The structure is complicated by disorder shown by one outer sphere nitrate ion and a MeOH solvent molecule; however, the inner sphere structure about the Er(III) is well-defined. The Er(III) ion is coordinated with two ligands, **5**, and two nitrate ions. The Er ion resides on a crystallographic 2-fold axis so that one DBF ligand and one nitrate ion in the inner sphere are related to the second ligand and nitrate by the 2-fold axis. Both molecules of **5** are chelated in a bidentate POP′O′ mode with Er−O bond lengths identical with those found in $[Er(\mathbf{4})(NO_3)_3(CH_3CN)]$, and the nitrate ions are bidentate. The eight inner sphere O-atoms generate a bidisphenoid coordination polyhedron. The DBF O-atoms are closer to the Er(III) ion but still well removed, 3.639 Å, and nonbonding. Here too, the base strength of the DBF O-atom is apparently so weak that it is not able to offset the strain energy developed in forming a tridentate chelate interaction.

Solvent Extraction. The solvent extraction properties of **4** and **5** toward Am(III) and Eu(III) in aqueous nitric acid solutions were investigated and compared to the well studied TRUEX extractant, *n*-octyl(phenyl)-*N*,*N*-diisobutylcarbamoylmethylphosphine oxide (OΦDiBCMPO = **CMPO**).[62] Both **4** and **5** are insoluble in the preferred organic phase extraction solvent, dodecane. Therefore, the distribution ratios, $D = [M_{org}/M_{aq}]$, for all three compounds were measured under the same conditions, as a function of the concentration of nitric acid, by using 0.01 M solutions of each in 1,2-dichloroethane (DCE). The variations of D with increasing $[HNO_3]$ are summarized in Figure 15. All three molecules show the unique property wherein the respective D's increase with increasing nitric acid concentration. Both **4** and **CMPO** reach their maximum D value at ∼1 M $[HNO_3]$ and then begin to decrease with further increases in $[HNO_3]$. This probably results from competing protonation of the phosphine oxide donor sites at high acid concentrations.[63] It is also apparent that the D's for **4** at all acid concentrations are significantly smaller than those for the **CMPO** ligand, and this is consistent with the trial spectrophotometric titration analysis data for **4** with La(III) in aqueous solution. In contrast, the maximum D values for extraction of both Am(III) and Eu(III) by **5** are reached at significantly higher nitric acid concentration, ∼5 M compared with ∼1 M with **4**. It is also clear from Figure 15 that **5** is a stronger extractant for both

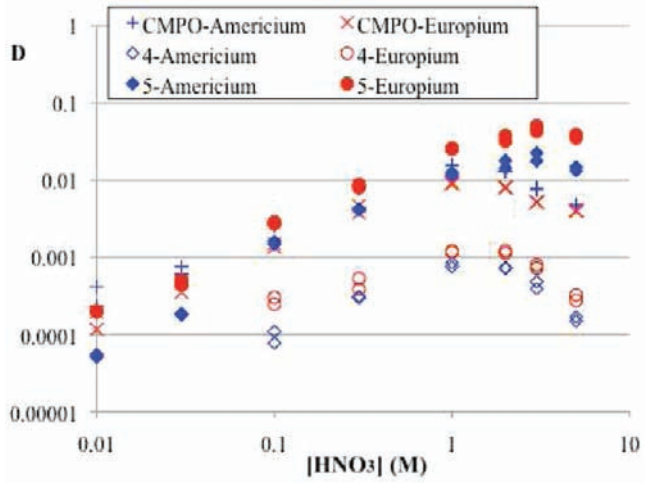

Figure 15. Americium and europium distribution ratios as a function of the initial nitric acid concentration. Organic phase: **4**, **5**, or **CMPO** at 10 mM in 1,2-DCE. Aqueous phase: trace ^{241}Am and 0.1 mM of europium nitrate in nitric acid. O/A = 1, T = 25 °C.

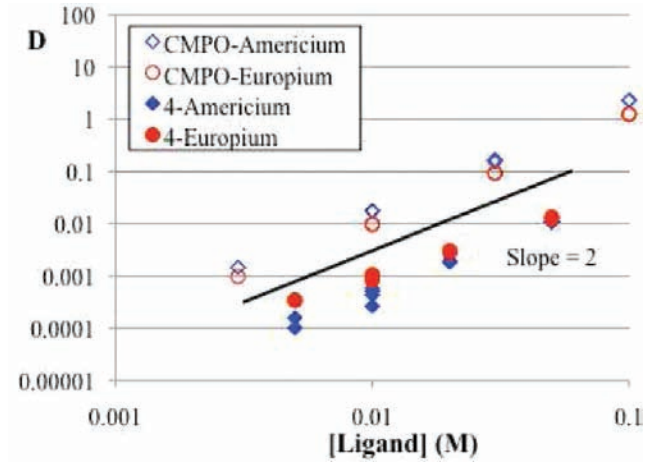

Figure 16. Americium and europium distribution ratios as a function of the initial ligand concentration. Organic phase: variable concentrations of **4** or CMPO in 1,2-DCE. Aqueous phase: trace ^{241}Am and 0.1 mM of europium nitrate in 1 M nitric acid. O/A = 1, T = 25 °C.

Eu(III) and Am(III) than **4** at all acid concentrations. This observation is consistent with the MM computed strain energy analysis that indicated lower ligand strain and better donor vector convergence for **5** compared to **4**. It is interesting that **5**, under identical conditions, appears to be a slightly better extractant than **CMPO** for Am(III) and Eu(III) in HNO_3 solutions above 0.5 M. This suggests that further comparative studies with more hydrocarbon soluble derivatives of **5**, **CMPO**, and **NOPOPO** are warranted. Lastly, it is noted that, under the conditions used for this study, **5** has a small preference to bind Eu(III) over Am(III) (α = 2.3 at 3 M HNO_3). The opposite is typically true with **CMPO** extractions of Am(III) and Eu(III).[63]

The ligand dependencies on D's for **4** and **CMPO** in DCE at constant nitric acid concentration (1 M) were also examined for both Am(III) and Eu(III) extractions, and the data are summarized in Figure 16. The ligand dependency for **5** was not measured in this study because of its more limited solubility range in DCE. From slope analyses, it is deduced that two molecules (slope = 2) of both **4** and **CMPO** are involved in

dx.doi.org/10.1021/ic300301d | Inorg. Chem. 2012, 51, 6667−6681

their extraction complexes. It can also be seen from Figure 16 that **CMPO** is the stronger extractant of this pair at all ligand concentrations studied. These results also encourage development of hydrocarbon solvent soluble analogues of **5** for additional detailed nitric acid extraction and ligand dependency extraction analyses, and those activities are in progress.

CONCLUSIONS

A high yield synthesis for the trifunctional ligand 4,6-bis(diphenylphosphinoylmethyl)dibenzofuran, **4**, has been developed, and ligand strain energies for potential bidentate POP′O′ and tridentate POP′O′O″ chelate interactions have been assessed with molecular mechanics calculations. In addition, a synthesis for 4,6-bis(diphenylphosphinoyl)dibenzofuran, **5**, has also been devised, and the strain energies for bidentate and tridentate chelate structures computed and compared with values obtained for **4** and NOPOPO. For both **4** and **5**, the strain energy is greater for the tridentate structure relative to the bidentate structure. Subsequent combinations of the ligands with several trivalent metal nitrates and Pu(IV) chloride produced coordination complexes for which single crystal X-ray diffraction structure determinations reveal formation of 1:1 and 2:1 complexes. In all cases **4** and **5** are found to act as bidentate POP′O′ chelates. Consistent with the computational analyses, no examples were isolated and structurally characterized where **4** or **5** adopt tridentate or metal bridged structures. This suggests that the DBF fragment O-atom is not a sufficiently strong donor site to offset the strain energy encountered in forming tridentate structures such as suggested for the acyclic analogue of **5**, 1,5-bis(diphenylphosphinoyl)-3-oxapentane.[64] A survey of the extraction performance of **4** and **5** in 1,2-DCE indicates that **5** is a stronger extractant for Am(III) and Eu(III) than **4** at all nitric acid concentrations studied (0.01−6 M) and slightly stronger than **CMPO** at nitric acid concentrations >1M. Further development of dialkyl and alkyl(aryl) phosphine oxide analogues of **5** are underway that will provide additional insight into the complexation and extraction performances of this ligand.

ASSOCIATED CONTENT

Supporting Information

Selected IR, vis−UV, and NMR spectra, CIF files for the crystal structures, PCModel input files for NOPOPO, **4** and **5**. This material is available free of charge via the Internet at http://pubs.acs.org. X-ray data have also been deposited with the Cambridge Crystallographic Data Centre with the deposition numbers 833444 (**4**·MeOH), 833445 (**4**·2H_2O), 833446 (**4**·H_2O), 833447 [Pr(**4**)$(NO_3)_3(CH_3CN)$]·0.5(CH_3CN), 833448 [Er(**4**)-$(NO_3)_3(CH_3CN)$]·(CH_3CN), 833449 [In(**4**)$(NO_3)_3$], 833450 [Nd$(\mathbf{4})_2(NO_3)_2]_2(NO_3)_2\cdot(H_2O)\cdot4(CH_3OH)$, 833451 {[Er-$(\mathbf{5})_2(NO_3)_2](NO_3)\cdot4(CH_3OH)\}_{0.5}$, and 833452 (**5**). These files may be accessed free of charge at http://www.ccdc.cam.ac.uk/conts/retrieving.html.

AUTHOR INFORMATION

Corresponding Author

*E-mail: rtpaine@unm.edu (R.T.P.); gaunt@lanl.gov (A.J.G.).

Notes

The authors declare no competing financial interest.

ACKNOWLEDGMENTS

The authors thank Professor R.D. Hancock and his group for their efforts to obtain aqueous solution formation constant data for **4** in combination with La(III). Financial support for this study at the University of New Mexico was provided by the Division of Chemical Sciences, Geosciences and Biosciences, Office of Basic Energy Sciences, U.S. Department of Energy (Grant DE-FG02-03ER15419 (R.T.P)). In addition, funds from the National Science Foundation assisted with the purchases of the X-ray diffractometer (CHE-0443580) and NMR spectrometers (CHE-0840523 and −0946690). B.P.H. and L.H.D. acknowledge support from the Division of Chemical Sciences, Geosciences and Biosciences, Office of Basic Energy Sciences, U.S. Department of Energy. A.J.G. and S.D.R. thank the U.S. Department of Energy, Office of Science, Early Career Research Program (contract DE-AC52-06NA25396). R.T.P. wishes to thank Prof. R. G. Bergman and Dr. V. Chan for unpublished details regarding the synthesis of **3**.

REFERENCES

(1) Haenel, M. W.; Jakubik, D.; Rothenberger, E.; Schroth, G. *Chem. Ber.* **1991**, *124*, 1705−1710.
(2) Kranenburg, M.; van der Burgt, Y. E. M.; Kamer, P. C. J.; van Leeumen, P. W. N. M.; Govbitz, K.; Fraamje, J. *Organometallics* **1995**, *14*, 3081−3089.
(3) Vogl, E. M.; Bruckmann, J.; Krüger, C.; Haenel, M. W. *J. Organomet. Chem.* **1996**, *520*, 249−252.
(4) Vogl, E. M.; Bruckmann, J.; Kessler, M.; Krüger, C.; Haenel, M. W. *Chem. Ber.* **1997**, *130*, 1315−1319.
(5) Hlavinka, M. L.; Hagadorn, J. R. *Chem. Commun.* **2003**, 2686−2687.
(6) Skar, M. L.; Svendsen, J. S. *Tetrahedron* **1997**, *53*, 17425−17437.
(7) (a) Kanemasa, S.; Oderaotoshi, Y.; Yamamoto, H.; Tanaka, J.; Wada, E. *J. Org. Chem.* **1997**, *62*, 6454−6455. (b) Kanemasa, S.; Oderaotoshi, Y.; Sakaguchi, S.; Yamamoto, H.; Tanaka, J.; Wada, E.; Curran, D. P. *J. Am. Chem. Soc.* **1998**, *120*, 3074−3088.
(8) Deng, Y.; Chang, C. J.; Nocera, D. G. *J. Am. Chem. Soc.* **2000**, *122*, 410−411.
(9) Kaul, R.; Deechongkit, S.; Kelly, J. W. *J. Am. Chem. Soc.* **2002**, *124*, 11900−11907.
(10) Kuang, S.-M.; Fanwick, P. E.; Walton, R. A. *Inorg. Chem.* **2002**, *41*, 405−412.
(11) Caradoc-Davies, P. L.; Hanton, L. R. *Dalton Trans.* **2003**, 1754−1758.
(12) Pintado-Alba, A.; de la Riva, H.; Nieuwhuyzen, M.; Bautista, D.; Raithby, P. R.; Sparkes, H. A.; Teat, S. J.; López-de-Luzuriaga, J. M.; Lagunas, C. M. *Dalton Trans.* **2004**, 3459−3467.
(13) Porter, R. M.; Danopoulos, A. A. *Polyhedron* **2006**, *25*, 859−863.
(14) De la Riva, H.; Nieuwhuyzen, M.; Fierro, C. M.; Raithby, P. R.; Male, L.; Lagunas, M. C. *Inorg. Chem.* **2006**, *45*, 1418−1420.
(15) Han, C.; Xie, G.; Li, J.; Zhang, Z.; Xu, H.; Dend, Z.; Zhao, Y.; Yan, P.; Liu, S. *Chem.—Eur. J.* **2011**, *17*, 8947−8956.
(16) Robbins, T. A.; Cram, D. J. *J. Chem. Soc., Chem. Commun.* **1995**, 1515−1516.
(17) Agbaria, K.; Biali, S. E. *J. Org. Chem.* **2001**, *66*, 5482−5489.
(18) Li, F.; Delgado, A.; Coelho, A.; Drew, M. G. B.; Félix, V. *Tetrahedron* **2006**, *62*, 8550−8558.
(19) Li, F.; Delgado, R.; Drew, M. G. B.; Félix, V. *Dalton Trans.* **2006**, 5396−5403.
(20) Li, F.; Li, L.; Delgado, R.; Drew, M. G. B.; Félix, V. *Dalton Trans.* **2007**, 1316−1324.
(21) McCabe, D. J.; Russell, A. A.; Karthikeyan, S.; Paine, R. T.; Ryan, R. R.; Smith, B. *Inorg. Chem.* **1987**, *26*, 1230−1235.
(22) Conary, G. S.; Russell, A. A.; Paine, R. T.; Hall, J. H.; Ryan, R. R. *Inorg. Chem.* **1988**, *27*, 3242−3245.

(23) Russell, A. A.; Meline, R. L.; Duesler, E. N.; Paine, R. T. *Inorg. Chim. Acta* **1995**, *231*, 1−5.
(24) Rapko, B. M.; Duesler, E. N.; Smith, P. H.; Paine, R. T.; Ryan, R. R. *Inorg. Chem.* **1993**, *32*, 2164−2174.
(25) Engelhardt, U.; Rapko, B. M.; Duesler, E. N.; Frutos, D.; Paine, R. T. *Polyhedron* **1995**, *14*, 2361−2369.
(26) Bond, E. M.; Duesler, E. N.; Paine, R. T.; Neu, M. P.; Matonic, J. H.; Scott, B. L. *Inorg. Chem.* **2000**, *39*, 4152−4155.
(27) Bond, E. M.; Duesler, E. N.; Paine, R. T.; Nöth, H. *Polyhedron* **2000**, *19*, 2135−2140.
(28) Gan, X.-M.; Duesler, E. N.; Paine, R. T. *Inorg. Chem.* **2001**, *40*, 4420−4427.
(29) Matonic, J. H.; Enriquez, A. E.; Scott, B. L.; Paine, R. T.; Neu, M. P. *Nucl. Sci. Tech.* **2002**, *3*, 100−105.
(30) Gan, X.-M.; Paine, R. T.; Duesler, E. N.; Nöth, H. *Dalton Trans.* **2003**, 153−159.
(31) Gan, X.-M.; Rapko, B. M.; Duesler, E. N.; Binyamin, I.; Paine, R. T.; Hay, B. P. *Polyhedron* **2005**, *24*, 469−474.
(32) Pailloux, S.; Shirima, C. E.; Ray, A. D.; Duesler, E. N.; Paine, R. T.; Klaehn, J. R.; McIlwain, M. E.; Hay, B. P. *Inorg. Chem.* **2009**, *48*, 3104−3113.
(33) Pailloux, S.; Shirima, C. E.; Ray, A. D.; Duesler, E. N.; Smith, K. A.; Paine, R. T.; Klaehn, J. R.; McIlwain, M. E.; Hay, B. P. *Dalton Trans.* **2009**, 7486−7493.
(34) Gan, X.-M.; Binyamin, I.; Rapko, B. M.; Fox, J.; Duesler, E. N.; Paine, R. T. *Polyhedron* **2006**, *25*, 3387−3392.
(35) Gan, X.-M.; Duesler, E. N.; Parveen, S.; Paine, R. T. *Dalton Trans.* **2003**, 4704−4708.
(36) Binyamin, I.; Pailloux, S.; Duesler, E. N.; Rapko, B. M.; Paine, R. T. *Inorg. Chem.* **2006**, *45*, 5886−5892.
(37) Binyamin, I.; Pailloux, S.; Hay, B. P.; Rapko, B. M.; Duesler, E. N.; Paine, R. T. *J. Heterocycl. Chem.* **2007**, *44*, 99−103.
(38) Bond, E. M.; Engelhardt, U.; Deere, T. P.; Rapko, B. M.; Paine, R. T. *Solvent Extr. Ion Exch.* **1997**, *15*, 381−400.
(39) Bond, E. M.; Engelhardt, U.; Deere, T. P.; Rapko, B. M.; Paine, R. T. *Solvent Extr. Ion Exch.* **1998**, *16*, 967−983.
(40) Nash, K. L.; Lavallette, C.; Borkowski, M.; Paine, R. T.; Gan, X.-M. *Inorg. Chem.* **2002**, *41*, 5849−5858.
(41) Sulakova, J.; Paine, R. T.; Chakravarty, M.; Nash, K. L. *Sep. Sci. Technol.*, submitted for publication.
(42) *SAINT + 7.01, 2003 (UNM), SAINT+ 7.06, 2003 (LANL)*; Bruker AXS, Inc.: Madison, WI.
(43) Sheldrick, G. M. *SADABS 2.10, 2003 (UNM), SADABS 2.03, 2001 (LANL)*; University of Göttingen: Göttingen, Germany.
(44) *SHELXTL*, 6.14; Bruker AXS, Inc.: Madison, WI, 2001.
(45) van der Sluis, P.; Spek, A. L. *Acta Crystallogr.* **1990**, *A46*, 194−201.
(46) (a) Allinger, N. L.; Yuh, Y.-H.; Lii, J.-H. *J. Am. Chem. Soc.* **1989**, *111*, 8551−8566. (b) Lii, J.-H.; Allinger, N. L. *J. Am. Chem. Soc.* **1989**, *111*, 8566−8575. (c) Lii, J.-H.; Allinger, N. L. *J. Am. Chem. Soc.* **1989**, *111*, 8576−8582.
(47) Hay, B. P. *Coord. Chem. Rev.* **1993**, *126*, 177−236.
(48) *PCModel*, version 9.3; Serena Software: Bloomington, IN.
(49) The syntheses for **2** and **3** are based upon unpublished procedures: Chan, V. S.; Bergman, R. G., private communication. Full details of the syntheses as employed in the present study are summarized in the Experimental Section.
(50) Elemental analyses (CHN) for the ligand **4** and its metal complexes were performed on multiple samples. Unfortunately, in some cases agreement with proposed compositions is not within ±0.4%. Scatter in replicate determinations suggests that some of the problem resides with difficulty in the analysis methodology. In addition, single crystal samples of complexes readily lose some lattice solvent that results in variable and low CH determinations. Analyses for noncrystalline samples of $[In(\mathbf{4})(NO_3)_3]$ and $[Er(\mathbf{4})(NO_3)_3]$ suggest formation of mixtures of 1:1 and 2:1 complexes.
(51) Even when computed in the absence of other factors, such as the presence of auxiliary inner-sphere ligation and counter-ions, outer-sphere solvation, etc., ligand strain energies have been successfully used to correlate ligand structure with metal ion binding affinity in a number of systems. (a) Hay, B. P.; Rustad, J. R.; Hostetler, C. J. *J. Am. Chem. Soc.* **1993**, *115*, 11158−11164. (b) Hay, B. P.; Zhang, D.; Rustad, J. R. *Inorg. Chem.* **1996**, *35*, 2650−2658. (c) Dietz, M. L.; Bond, A. H.; Hay, B. P.; Chiarizia, R.; Huber, V. J.; Herlinger, A. W. *Chem. Commun.* **1999**, 1177−1178. (d) Hay, B. P.; Dixon, D. A.; Vargas, R.; Garza, J.; Raymond, K. N. *Inorg. Chem.* **2001**, *40*, 3922−3935. (e) Lumetta, G. J.; Rapko, B. M.; Garza, P. A.; Hay, B. P.; Gilbertson, R. D.; Weakley, T. J. R.; Hutchison, J. E. *J. Am. Chem. Soc.* **2002**, *124*, 5644−5645. (f) Hay, B. P.; Oliferenko, A. A.; Uddin, J.; Zhang, C.; Firman, T. K. *J. Am. Chem. Soc.* **2005**, *127*, 17043−17053.
(52) Hay, B. P.; Hancock, R. D. *Coord. Chem. Rev.* **2001**, *212*, 61−78.
(53) (a) Cambridge Structural Database, November, 2012. (b) Allen, F. H. *Acta Crystallogr.* **2002**, *B58*, 380−388. (c) Bruno, I. J.; Cole, J. C.; Edgington, P. R.; Kessler, M.; Macrae, C. F.; McCabe, P.; Pearson, J.; Taylor, R. *Acta Crystallogr.* **2002**, *B58*, 389−397.
(54) Junk, P. C.; Skelton, B. W.; White, A. H. *Aust. J. Chem.* **2006**, *59*, 147−154.
(55) Peppe, C.; Nobrega, J. A.; Hernandes, M. Z.; Longo, R. L.; Tuck, D. G. *J. Organomet. Chem.* **2001**, *626*, 68−75.
(56) Robinson, W. T.; Wilkins, C. J.; Zeying, Z. *J. Chem. Soc., Dalton Trans.* **1990**, 219−227.
(57) Ryan, J. L.; Jorgensen, C. K. *Mol. Phys.* **1963**, *7*, 17−29.
(58) Nikitenko, S. I.; Moisy, P. *Inorg. Chem.* **2006**, *45*, 1235−1242.
(59) Berthon, C.; Boubals, N.; Charusnikova, I. A.; Collison, D.; Cornet, S. M.; Den Auwer, C.; Gaunt, A. J.; Kaltsoyannis, N.; May, I.; Petit, S.; Redmond, M. P.; Reilly, S. D.; Scott, B. L. *Inorg. Chem.* **2010**, *49*, 9554−9562.
(60) Matonic, J. H.; Neu, M. P.; Enriquez, A. E.; Paine, R. T.; Scott, B. L. *J. Chem. Soc., Dalton Trans.* **2002**, 400−405.
(61) Shannon, R. D.; Prewitt, C. T. *Acta Crystallogr.* **1969**, *B25*, 925−930.
(62) Horwitz, E. P.; Kalina, D. G.; Diamond, H.; Vandegrift, G. F.; Schulz, W. W. *Solvent Extr. Ion. Exch.* **1985**, *3*, 75−109.
(63) Horwitz, E. P.; Martin, K. A.; Diamond, H.; Kaplan, L. *Solvent Extr. Ion Exch.* **1986**, *4*, 449−494.
(64) (a) Turanov, A. N.; Karandashev, V. K.; Baulin, V. E. *Solvent Extr. Ion Exch.* **1999**, *17*, 1423−1444. (b) Turanov, A. N.; Karandashev, V. K.; Baulin, V. E.; Yarkevich, A. N.; Safronova, Z. V. *Solvent Extr. Ion Exch.* **2009**, *27*, 551−578.